Electronic Supplementary Material (ESI) for CrystEngComm.

Electronic Supplementary Information

Dimesitylboryl Functionalised Cyanostilbene Derivatives of Phenothiazine: Distinctive Polymorphism Dependent Emission and Mechanofluorochromism

C. Arivazhagan, Partha Malakar, R. Jagan, Edamana Prasad* and Sundargopal Ghosh*
Department of Chemistry, Indian Institute of Technology Madras, Chennai 600 036, India.

Table of Contents

I. Experimental Section

Materials and methods

Mes_2BF,[1] and 7-Bromo-10-ethyl-10H-phenothiazine-3-carbaldehyde[2] were prepared according to known methods. All other starting materials were purchased from commercials sources and used without further purification. For photophysical studies HPLC grade solvents were used. All synthetic reactions were performed under an argon atmosphere using standard Schlenk line techniques. ^{1}H, $^{13}C\{^{1}H\}$ and $^{11}B\{^{1}H\}$ NMR spectra were recorded on a Bruker Avance 500 MHz (^{1}H, 500 MHz; ^{13}C, 125 MHz; ^{11}B, 160 MHz) or Bruker Avance III 400 MHz (^{1}H, 400 MHz; ^{13}C, 100 MHz; ^{11}B, 128 MHz) NMR spectrometer. HRMS spectra were recorded on Qtof Micro YA263 HRMS instrument.

General photophysical and other measurements

All measurements were made in standard quartz cuvettes (1 cm $\times$ 1 cm). UV-visible absorption spectra were recorded using Jasco V-650, UV-visible spectrophotometer. The emission and excitation spectra were recorded using Jasco FP-6300 or Horiba Jobin Yvon Fluoromax-4 spectrometers. Timeresolved fluorescence measurements were performed on Horiba Jobin Yvon TCSPC lifetime instrument in a time-correlated, single-photon counting arrangement. 405 nm nano-LED was used as light source. The decay data were analyzed using IBH software. A value of χ^2, $0.99 \leq \chi^2 \leq 1.3$ was considered as a good fit.

Single Crystal X-ray diffraction

X-ray diffraction data for the crystals **3YC**, **3RC** and **4** was collected using Bruker Kappa apexII CCD Single Crystal Diffractometer, equipped with graphite monochromated Mo Kα (λ=0.71078Å) radiation. Data collection was carried out at 293 K using ω-ϕ scan modes. The collected frames were integrated followed by Lorentz and Polarization correction using the program SAINT-APEXII software.[3] Multi-scan absorption correction has been employed for the data using SADABS program.[4] The molecular structure was solved by direct methods procedure using SHELXS-2014/7.[5] Initially isotropic refinements of non-hydrogen atoms were carried out followed by full-matrix least squares refinement with anisotropic thermal parameters for non-hydrogen atoms through SHELXL-2014/7 program. The hydrogen atoms associated with the carbon atoms were identified from the difference electron density map and were allowed to ride on the parent atom using suitable constraint, with distance 0.93Å(for aromatic CH) and 0.96Å(for CH_3) and thermal displacement of $U_{iso}(H) = 1.2U_{eq}(C)$ and $U_{iso}(H) = 1.5U_{eq}(C)$ respectively. Some of the disordered methyl hydrogen of **3YC** and **3RC** are fixed as riding hydrogens with two positions rotated from each other by 60˚ with equal occupancy of 0.5. All the interactions and molecular drawings were obtained using the program Mercury (ver. 3.9).

Theoretical studies

All calculations (DFT and TD-DFT) were carried out with the program package Gaussian 09 (Rev. C. 01)[6] and were performed on a parallel cluster system. The starting geometries for the calculations were those obtained by X-ray crystallography. The ground-state geometries were optimized without symmetry constraints using the B3LYP fuctional[7] in combination with the 6-31G(d) basis set.[8] The optimized geometries were confirmed to be local minima by performing frequency calculations and obtaining only positive (real) frequencies. Based on these optimized structures, the lowest-energy gas-phase vertical transitions were calculated (singlets, six states) by TD-DFT, using the Coulomb-attenuated functional CAM-B3LYP[9] in combination with the 6-31G(d). TD-DFT results were extracted and plotted using GaussSum 3.0 software.[10]

II. Syntheses of compounds 1-4

3-bromo-7-(5,5-dimethyl-1,3-dioxan-2-yl)-10-ethyl-10H-phenothiazine (1)

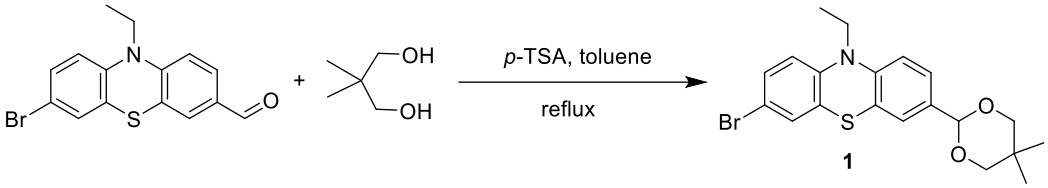

7-bromo-10-ethyl-10H-phenothiazine-3-carbaldehyde (12.50 g, 37.39 mmol), 2,2-methyl-1,3-propandiol (7.79 g ,74.79 mmol) and a catalytic amount of p-toluenesulfonic acid in toluene (150 mL) was refluxed for 4 h. The reaction mixture was allowed to reach room temperature, extracted with dichloromethane and washed with brine solution. The organic layer was dried over anhydrous Na_2SO_4 and the solvent was removed under vacuum. The crude product was purified by basic alumina column chromatography using 40% dichromethane in hexane yielding the product as colorless crystalline solid (11.64 g, 74 %).

^{1}H NMR (400 MHz, $CDCl_3$, δ): 7.25-7.27 (m, 2H), 7.17-7.2 (m, 2H), 6.80 (d, 1H, *J* = 8.2 Hz), 6.65 (d, 1H, *J* = 9.24 Hz), 5.28 (s, 1H), 3.84 (q, 2H, *J* = 6.9 Hz), 3.73 (d, 2H, *J* = 11.1 Hz), 3.6 (d, 2H, *J* = 10.7 Hz), 1.35 (t, 3H, *J* = 6.9 Hz), 1.26 (s, 3H), 0.77 (s, 3H)

^{13}C{^{1}H} NMR (100 MHz, $CDCl_3$, δ): 144.8, 144.0, 133.2, 129.8, 129.4, 126.5, 125.3, 125.2, 123.6, 116.1, 114.8, 114.2, 100.94, 77.6, 41.9, 30.1, 23.0, 21.8, 12.7.

7-(dimesitylboranyl)-10-ethyl-10H-phenothiazine-3-carbaldehyde, (2)

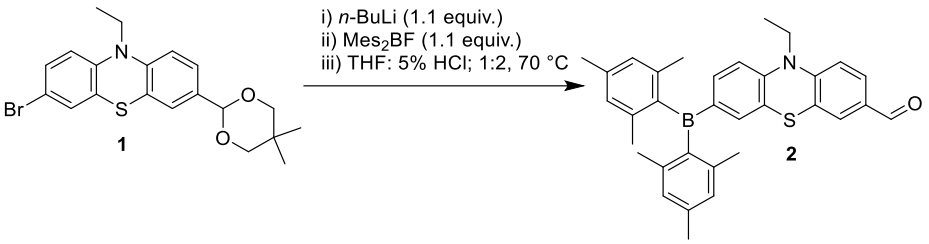

3-bromo-7-(5,5-dimethyl-1,3-dioxan-2-yl)-10-ethyl-10H-phenothiazine (11.64 g, 27.68 mmol) was dissolved in THF (150 mL), This solution was cooled to -78 °C, and *n*BuLi (19 mL, 30.45 mmol, 1.6 M in hexane) was added dropwise. The reaction mixture was allowed to stir 30 min and then Mes_2BF (8.16 g, 30.45 mmol) in THF (50 mL) was added at -78 °C dropwise. The color of the solution changed pale yellow to bright green. The reaction mixture slowly allowed to RT and then stirred overnight. The reaction mixture was reduced to one third of its volume and treated with 5% hydrochloric acid solution (THF: 5% HCl; 1:2) heated to 70 °C for 1 hour. During which time, greenish yellow precipitate formed. The reaction mixture allowed to reach room temperature and neutralized using an aqueous solution of $NaHCO_3$ and extracted with ether. In the separating funnel, green precipitate stayed on the orange color organic layer and clear aqueous layer was discarded. Orange color solution was discarded by decantation from top and the precipitate collected and washed three times with ether to yield compound **2** as bright green powder (6.35 g, 45.5 %). Column chromatography was not required as the product formed in good purity as checked by TLC and NMR.

^{1}H NMR (400 MHz, $CDCl_3$, δ): 9.78 (s, 1H), 7.62 (dd, 1H, *J* = 1.7, 8.5 Hz), 7.52 (d, 1H, *J* = 1.8 Hz), 7.3 (dd, 1H, *J* = 1.4, 8.2 Hz), 7.21 (d, 1H, *J* = 1.4 Hz), 6.91 (d, 1H, *J* = 8.4 Hz), 6.84 (s, 1H), 6.82 (s, 4H), 3.98 (q, 2H, *J* = 6.9 Hz), 2.31 (s, 6H), 2.02 (s, 12H), 1.46 (t, 3H, *J* = 6.9 Hz).
^{13}C{^{1}H} NMR (100 MHz, $CDCl_3$, δ): 190.0, 149.1, 146.3, 141.2, 140.7, 138.5, 137.2, 135.6, 131.3, 130.0, 128.2, 128.1, 124.3, 121.8, 114.6, 114.6, 42.7, 23.5, 21.2, 12.7.
^{11}B{^{1}H} NMR (160 MHz, $CDCl_3$, δ): 78.8.
HRMS: calcd. m/z for $C_{33}H_{35}BNOS^+$ $[M+H]^+$, 504.2532; found, 504.2531.

(Z)-2-(4-bromophenyl)-3-(7-(dimesitylboranyl)-10-ethyl-10H-phenothiazin-3-yl)acrylonitrile (3)

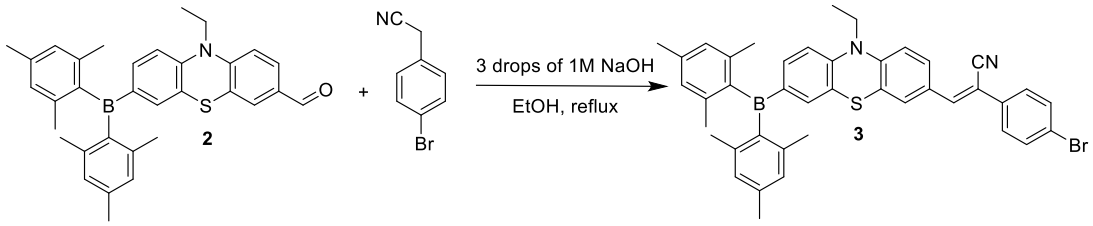

Compound **2** (503 mg, 1 mmol) and 4-bromophenyl acetonitrile (196 mg, 1 mmol) were mixed in 20 mL of ethanol. To this mixture three drops of 1N NaOH solution was added and refluxed vigorously for 4 h. The reaction mixture was allowed to cool to room temperature. Formed yellow precipitate was filtered through G4 frit. After column chromatography using silica gel with the eluent of 2% ethylacetate in hexane yielded the product as red colored solid (0.59 g, 86 %).

^{1}H NMR (400 MHz, $CDCl_3$, δ): 7.80 (dd, 1H, *J* = 2.0, 8.7 Hz), 7.48-7.55 (m, 4H), 7.45 (d, 1H, *J* = 2.1 Hz), 7.31-7.33 (m, 2H), 7.23 (d, 1H, *J* = 1.4 Hz), 6.88 (d, 1H, *J* = 8.6 Hz), 6.83 (s, 4H), 6.81 (s, 1H), 3.97 (q, 2H, *J* = 6.9 Hz), 2.32 (s, 6H), 2.04 (s, 12H), 1.46 (t, 3H, *J* = 6.9 Hz).

^{13}C{^{1}H} NMR (100 MHz, $CDCl_3$, δ): 146.7, 145.7, 141.3, 140.8, 140.7,140.1, 138.4, 137.3, 135.6, 133.6, 132.1, 128.5, 128.5, 128.2, 128.1, 127.2, 124.1, 122.9, 121.6, 118.0, 114.9, 114.3, 107.7, 42.5, 23.5, 21.25, 12.7.

^{11}B{^{1}H} NMR (160 MHz, $CDCl_3$, δ): 78.8.

HRMS: calcd. m/z for $C_{41}H_{39}BBrN_2S^+$ $[M+H]^+$, 681.2110; found, 681.2094.

(Z)-2-(4-bromophenyl)-3-(10-ethyl-10H-phenothiazin-3-yl)acrylonitrile (4)

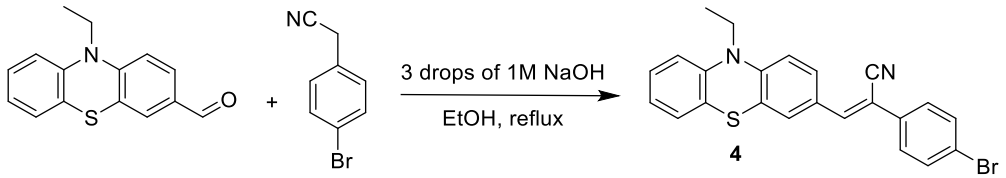

10-ethyl-phenothiazine-3-carbaldehyde (1.5 g, 5.87 mmol) and 4-bromophenyl acetonitrile (1.2 equiv.) were mixed in 30 mL of ethanol. To this mixture three drops of 1N NaOH solution were added and refluxed vigorously for 4 h. The reaction mixture was allowed to cool to room temperature. The yellow precipitate formed was filtered through G4 frit. After column chromatography using silica gel with the eluent of 2% ethylacetate in hexane yielded the product as red colored solid (2.1 g, 82.4 %).

^{1}H NMR (400 MHz, $CDCl_3$, δ): 7.66 (dd, 1H, *J* = 6.6, 10.8 Hz), 7.36-7.43 (m, 5H), 7.20 (s, 1H), 7.02-7.06 (m, 1H), 6.98 (dd, 1H, *J* = 1.5, 7.6 Hz), 6.83 (td, 1H, *J* = 1.0, 14.9 Hz), 6.73-6.77 (m, 2H), 3.82 (q, 2H, *J* = 6.9 Hz), 1.32 (t, 3H, *J* = 6.9 Hz).
^{13}C{^{1}H} NMR (100 MHz, $CDCl_3$, δ): 413.4, 141.0, 133.7, 132.1, 128.8, 128.3, 127.5, 127.5, 127.4, 127.4, 127.3, 127.2, 127.2, 127.1, 124.2, 123.1, 123.8, 118.0, 115.2, 114.7, 114.6, 107.2, 42.2, 12.8.
HRMS: calcd. m/z for $C_{23}H_{18}N_2SBr^+$ $[M+H]^+$, 433.0374; found, 433.0354.

Synthesis of different polymorphs of compound 3

500 mg of compound **3** was dissolved in 10 mL mixture of DCM and hexane in the ratio of 2/8 volume and kept at room temperature for 2 days. As shown in Fig. S1, different types of polymorphs formed. The solution was decanted and **3YA** was scratched from the inner surface of the test tube using semi-micro spatula. Whereas, **3YC** and **3RC** were separated using long needles. Using this technique, polymorphs **3YA** and **3RC** were separated in good amount. In order to collect good amount of **3YC**, the separated **3YC** from the test tube was seeded into the solution mixture (DCM and hexane, 2/8 volume ratio) in round bottom flask (Fig. S1, right). More **3YC** was formed in overnight, if any solution left was decanted and the crystals were isolated.

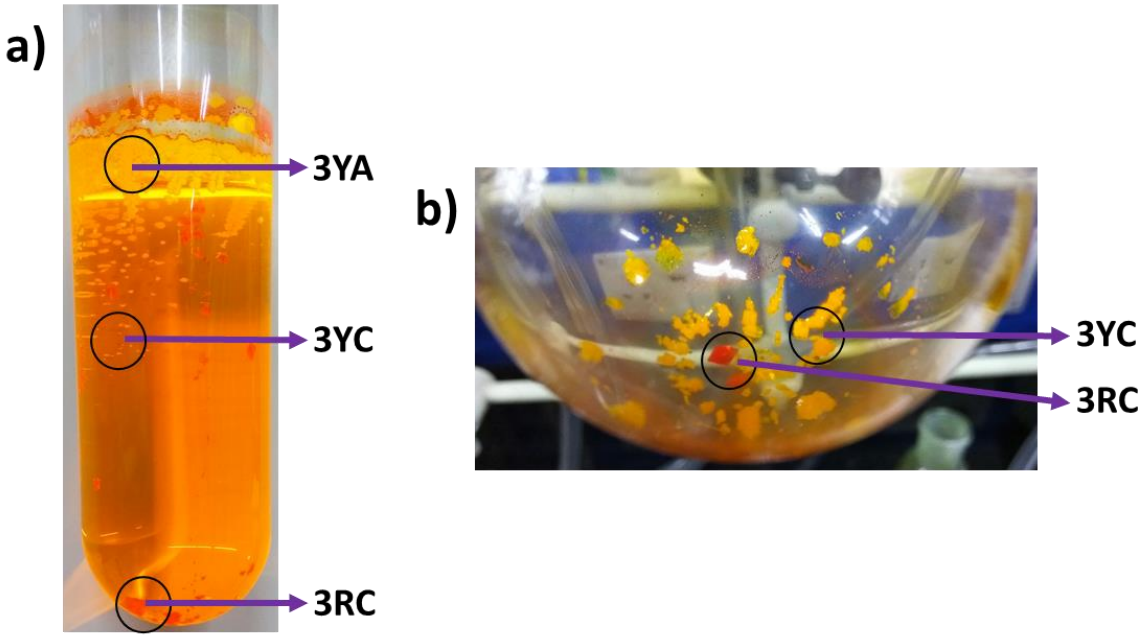

Fig. S1. Photograph of the preparation of different types of polymorphs of **3**. (a) in test tube (b) in round bottom flask.

III. Optical Properties

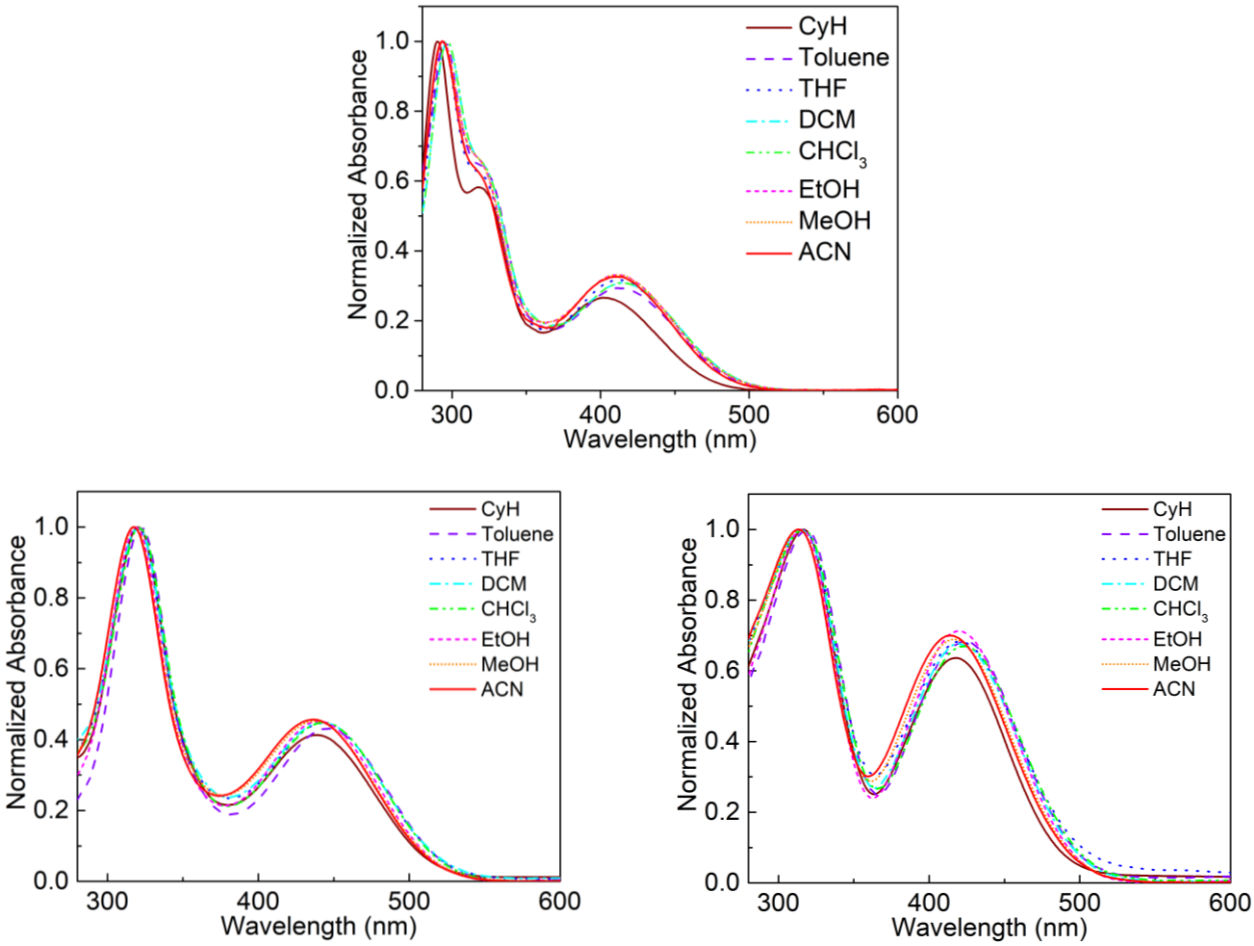

Fig. S2. Absorption spectra of compounds **2** (top), **3** (bottom left) and **4** (bottom right) in various solvents (10 μM)

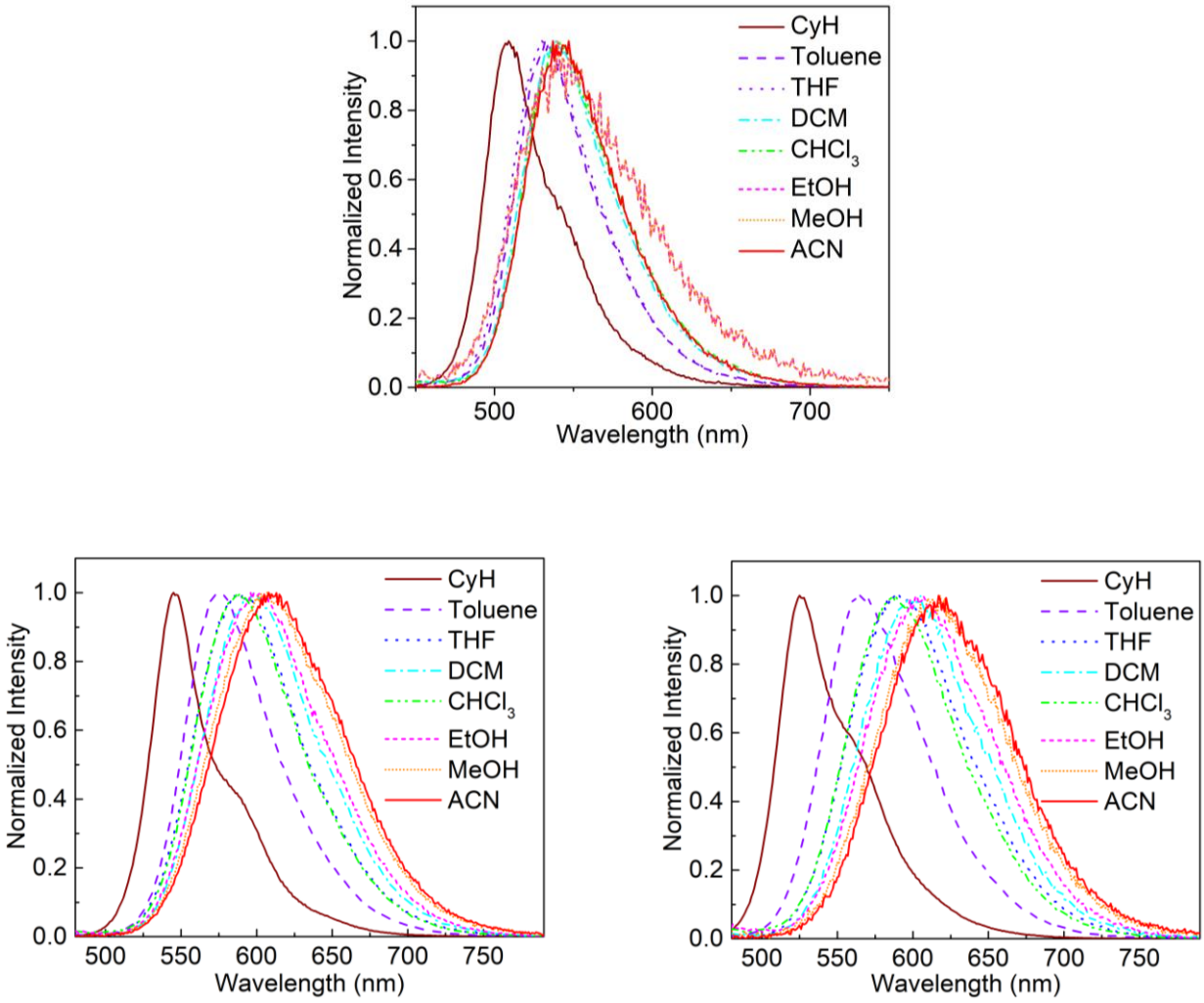

Fig. S3. Fluorescence spectra of compounds **2** (top), **3** (bottom left) and **4** (bottom right) in various solvents (10 μM). All spectra were recorded with the excitation wavelength of 400 nm.

Fig. S4. Fluorescence images of compounds **2** (top), **3** (bottom left) and **4** (bottom right) in solvents with different polarities under UV excitation at 365 nm.

Table S1. Photophysical properties of **2**, **3** and **4** in various solvents

Compound	Solvent	λ_{abs}/nm	λ_{em}/nm (Φ_F)[a]	Stokes shift/cm^{-1}
2	Cyclohexane	290, 318 (sh), 401	509 (0.59)	5291
	Toluene	295, 320 (sh), 412	532 (0.47)	5474
	THF	293, 319 (sh), 412	531 (0.51)	5439
	DCM	295, 320 (sh), 412	538 (0.43)	5445
	$CHCl_3$	296, 320 (sh), 415	540 (0.43)	5577
	EtOH	295, 320 (sh), 412	541 (0.04)	5579
	MeOH	294, 319 (sh), 411	540 (0.04)	5812
	MeCN	293, 318 (sh), 410	541 (0.43)	5905
3	Cyclohexane	320, 438	545 (0.43)	4482
	Toluene	322, 446	575 (0.30)	5030
	THF	320, 443	589 (0.27)	5595
	DCM	320, 443	598 (0.23)	5850
	$CHCl_3$	321, 443	588 (0.25)	5566
	EtOH	319, 440	600 (0.11)	6060
	MeOH	318, 437	607 (0.08)	6408
	MeCN	317, 436	610 (0.13)	6542
4	Cyclohexane	317, 417	525 (0.35)	4933
	Toluene	318, 424	566 (0.20)	5917
	THF	316, 419	590 (0.17)	6917
	DCM	314, 419	602 (0.13)	7255
	$CHCl_3$	316, 423	586 (0.12)	6575
	EtOH	315, 419	604 (0.06)	7310
	MeOH	313, 415	615 (0.03)	7836
	MeCN	313, 413	617 (0.07)	8005

[a]Quantum yields measured using fluorescein (0.1 M NaOH, Φ_F = 0.89) solution as reference.

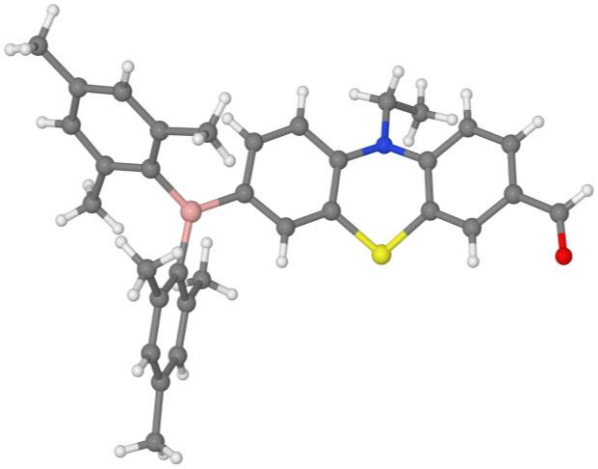

Figure S5. Ground state DFT optimized structure of **2**

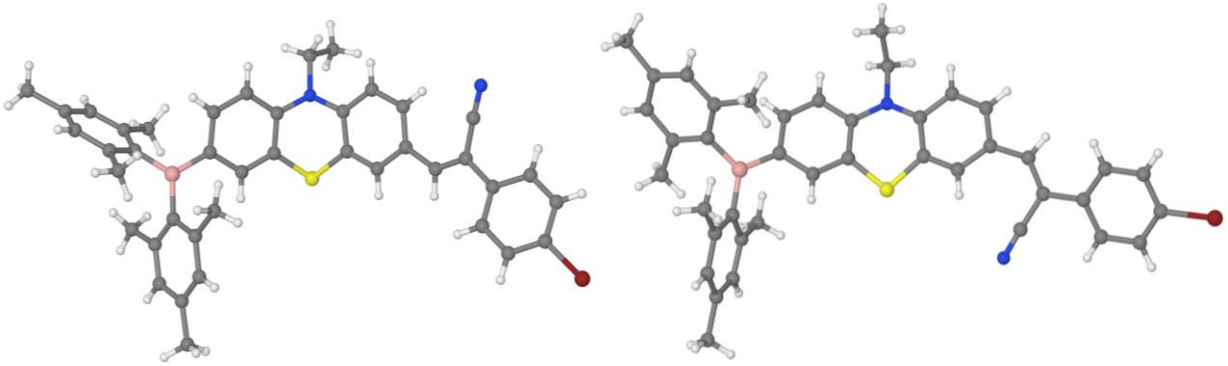

Figure S6. Ground state DFT optimized structure of **3YC** (left) and **3RC** (right)

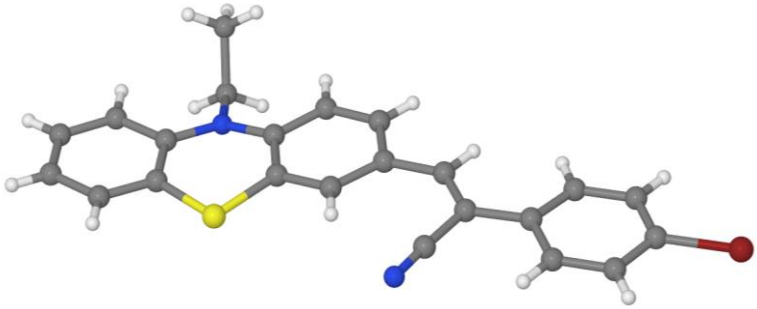

Fig. S7. Ground state DFT optimized structure of **4**

IV. DFT results

Compound **2**, ΔE = 3.62 eV (342.49 nm)		
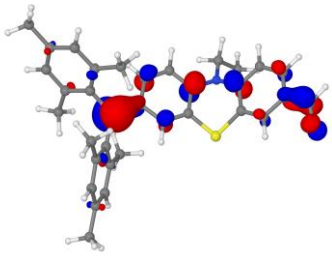	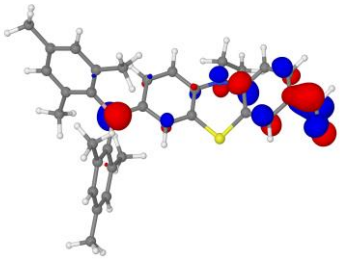	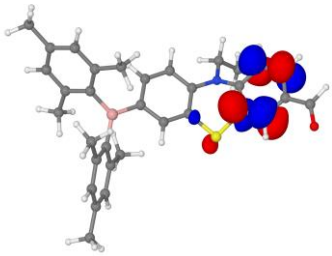
LUMO, -1.79 eV	LUMO+1, -1.50 eV	LUMO+2, -0.55 eV
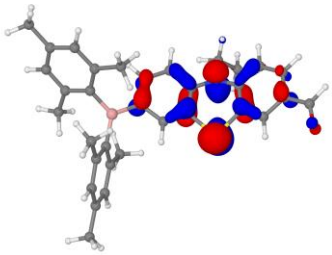	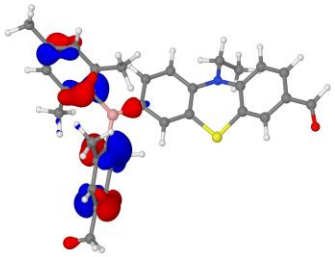	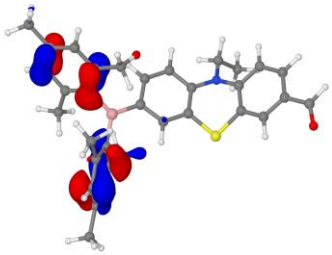
HOMO, -5.42 eV	HOMO-1, -6.02 eV	HOMO-2, -6.12 eV

Compound **3YC**, ΔE = 3.14 eV (394.85 nm)		
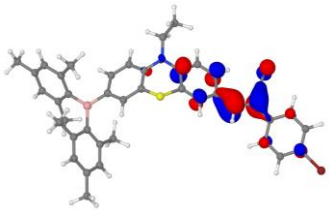	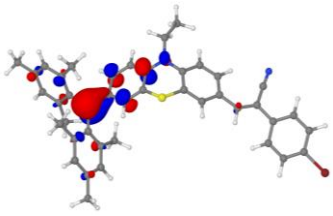	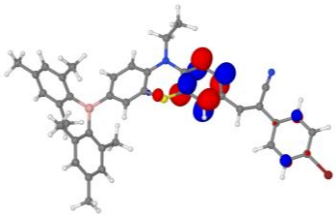
LUMO, -2.20 eV	LUMO+1, -1.68 eV	LUMO+2, -0.56 eV
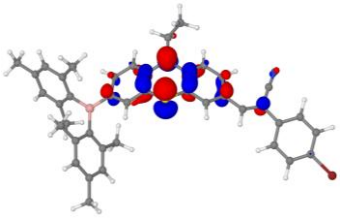	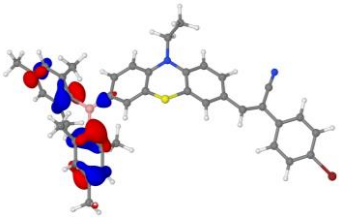	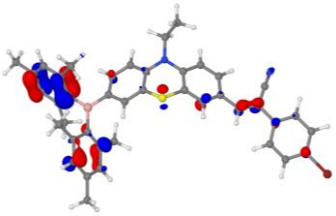
HOMO, -5.34 eV	HOMO-1, -6.07 eV	HOMO-2, -6.13 eV

Compound **3RC** ΔE = 2.97 eV (417.45 nm)		
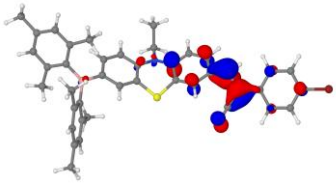	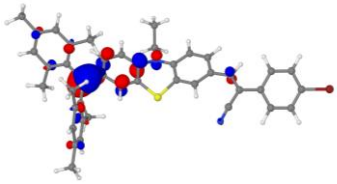	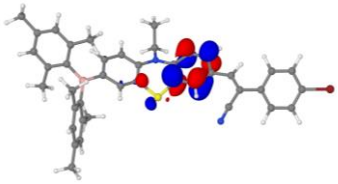
LUMO, -2.18 eV	LUMO+1, -1.62 eV	LUMO+2, 0.59 eV
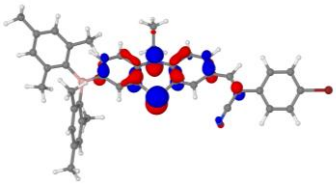	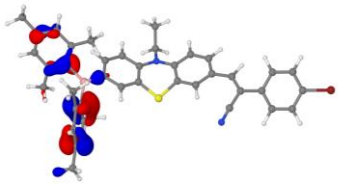	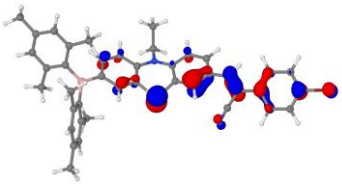
HOMO, -5.16 eV	HOMO-1, -6.00 eV	HOMO-2, -6.08 eV
Compound **4** ΔE = 3.02 eV (410.54 nm)		
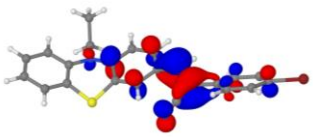	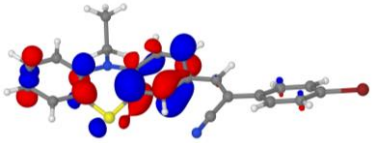	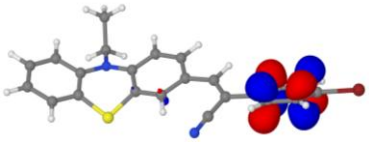
LUMO, -2.09 eV	LUMO+1, -0.62 eV	LUMO+2, -0.48 eV
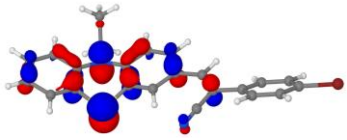	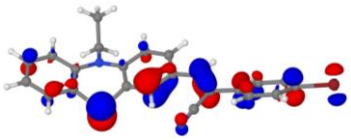	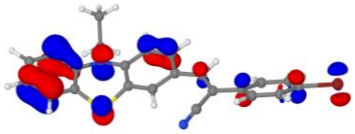
HOMO, -5.12 eV	HOMO-1, -6.06 eV	HOMO-2, -6.51 eV

Fig. S8. Frontier molecular orbitals of **2**-**4**

Table S2. TD-DFT calculated electronic transition configurations for **2**-**4** along with their corresponding excitation energies and oscillator strengths.[a]

Compounds	Excited State	Transition Configurations	Excitation Energy (nm, eV)	Oscillator Strengths
2	1	HOMO->LUMO (84%)	340.84 (3.63)	0.4248
	2	H-8->LUMO (25%), H-8->L+1 (50%)	308.42 (4.01)	0.0091
	3	H-1->LUMO (68%), H-1->L+1 (23%)	302.30 (4.10)	0.1394
	4	H-2->LUMO (17%), HOMO->L+1 (63%)	295.85 (4.19)	0.1638
	5	H-2->LUMO (46%), H-2->L+1 (15%), HOMO->L+1 (11%)	281.95 (4.39)	0.0787
	6	H-5->LUMO (22%), HOMO->L+2 (35%), HOMO->L+3 (15%)	276.98 (4.47)	0.0031
	7	H-3->LUMO (57%), H-3->L+1 (19%)	270.90 (4.57)	0.0824
	8	H-4->LUMO (56%), H-4->L+1 (20%)	266.63 (4.65)	0.0289
	9	H-5->LUMO (18%), H-5->L+1 (12%), HOMO->L+1 (11%), HOMO->L+2 (19%), HOMO->L+3 (11%)	262.12 (4.73)	0.078
	10	H-5->LUMO (23%), HOMO->L+3 (30%)	256.43 (4.83)	0.6173
3	1	HOMO->LUMO (88%)	402.49 (3.08)	0.9622
	2	HOMO->L+1 (68%)	323.98 (3.82)	0.2855
	3	H-2->LUMO (40%), H-1->L+1 (25%)	303.26 (4.08)	0.2561
	4	H-2->LUMO (26%), H-1->L+1 (50%)	302.19 (4.10)	0.4026
	5	H-3->L+1 (21%), HOMO->L+2 (49%)	290.21 (4.27)	0.3019
	6	H-3->L+1 (38%)	283.61 (4.37)	0.0333
	7	H-4->LUMO (11%), H-4->L+1 (48%)	271.92 (4.55)	0.0902
	8	H-6->L+1 (12%), H-4->L+1 (17%), HOMO->L+4 (13%)	268.02 (4.62)	0.0297
	9	H-5->LUMO (14%), H-5->L+1 (61%)	266.66 (4.64)	0.024
	10	H-6->LUMO (44%)	258.30 (4.80)	0.0816
4	1	HOMO->LUMO (98%)	479.12 (2.58)	0.5824
	2	H-1->LUMO (91%)	354.52 (3.49)	0.5748
	3	HOMO->L+1 (85%)	335.95 (3.69)	0.197
	4	H-2->LUMO (82%)	314.17 (3.94)	0.0419
	5	HOMO->L+3 (58%), HOMO->L+4 (28%)	301.99 (4.10)	0.0553
	6	HOMO->L+2 (84%)	295.05 (4.20)	0.0181
	7	HOMO->L+3 (20%), HOMO->L+4 (49%), HOMO->L+5 (13%)	288.05 (4.30)	0.0211
	8	H-4->LUMO (10%), H-3->LUMO (28%), HOMO->L+5 (41%)	278.12 (4.45)	0.0401
	9	H-5->LUMO (78%)	273.53 (4.53)	0.0052
	10	H-4->LUMO (72%)	271.98 (4.55)	0.0274

[a] Components with greater than 10 % contribution shown.

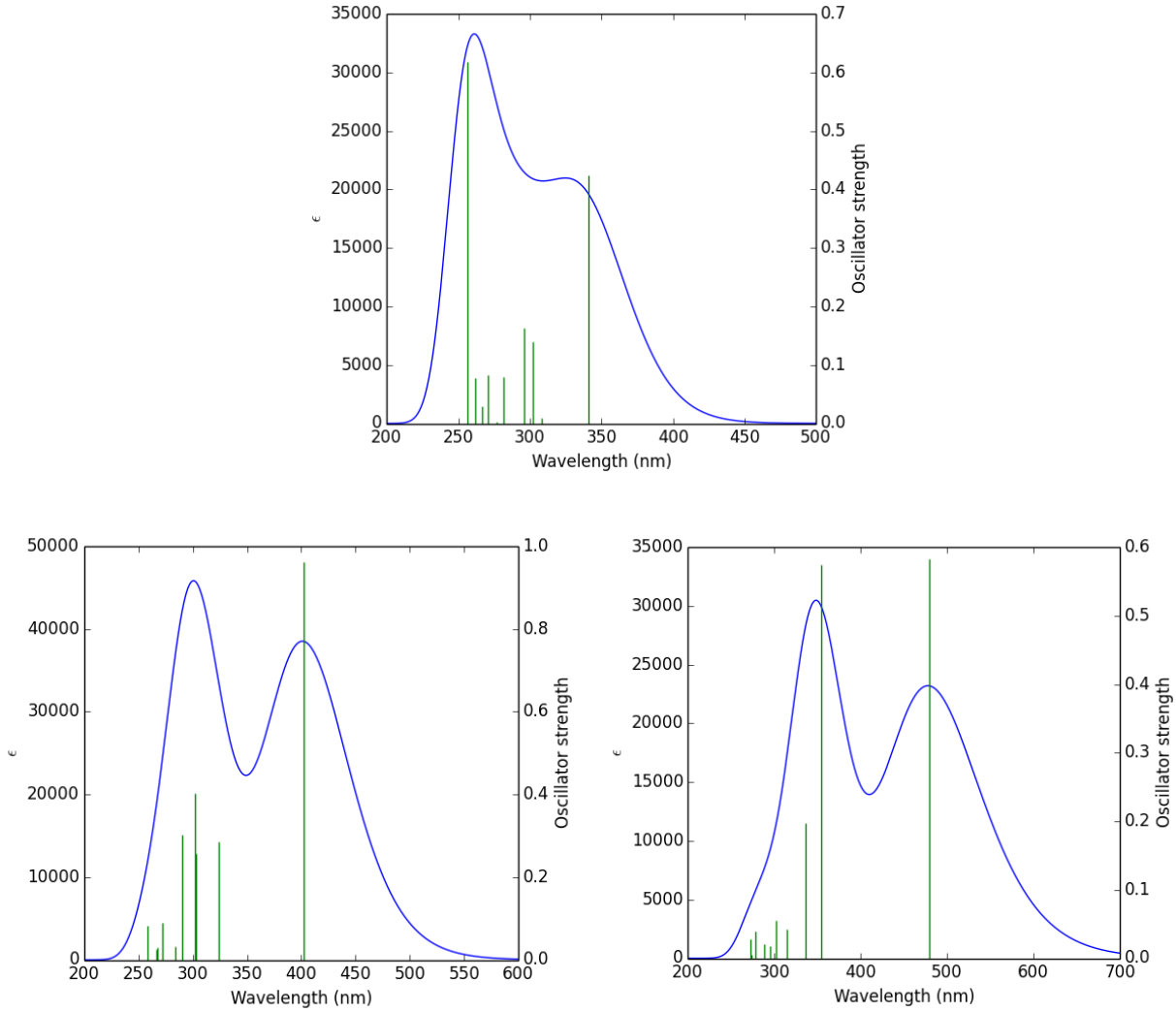

Fig. S9. Calculated absorption spectra of **2** (top), **3** (bottom left) and **4** (bottom right) (first 10 excited states); TD-CAM-B3LYP/6-31G(d) PCM=THF

V. Fluorescent Lifetime Studies

Table S3. Photophysical properties and fluorescence decay parameters of compounds (**2**-**4**) in cyclohexane solution[a]

Compounds	Absorption λ_{abs} [nm]	Fluorescence λ_{em} (Φ_F)[a] [nm]	Stokes shift [nm] ([cm^{-1}])	Lifetime $\langle\tau\rangle$[b] (ns)	K_r[c] (s^{-1})	K_{nr}[c] (s^{-1})
2	401	509 (0.59)	108 (5291)	6.4	0.9×10^8	0.6×10^8
3	438	545 (0.43)	107 (4482)	3.9	1.1×10^8	1.4×10^8
4	417	525 (0.35)	108 (4933)	2.6	1.3×10^8	2.5×10^8

[a] The fluorescence quantum yields measured using fluorescein (0.1 M NaOH, Φ_F = 0.89) solution as reference. [b] The average lifetime was calculated using the following equation: $\langle\tau\rangle = \alpha_1\tau_1 + \alpha_2\tau_2$. [c] The rate constants for radiative (k_r) and nonradiating decay (k_{nr}) were calculated from the Φ_F and τ values according to the formulae $k_r = \Phi_F/\tau$ and $k_{nr} = (1-\Phi_F)/\tau$.

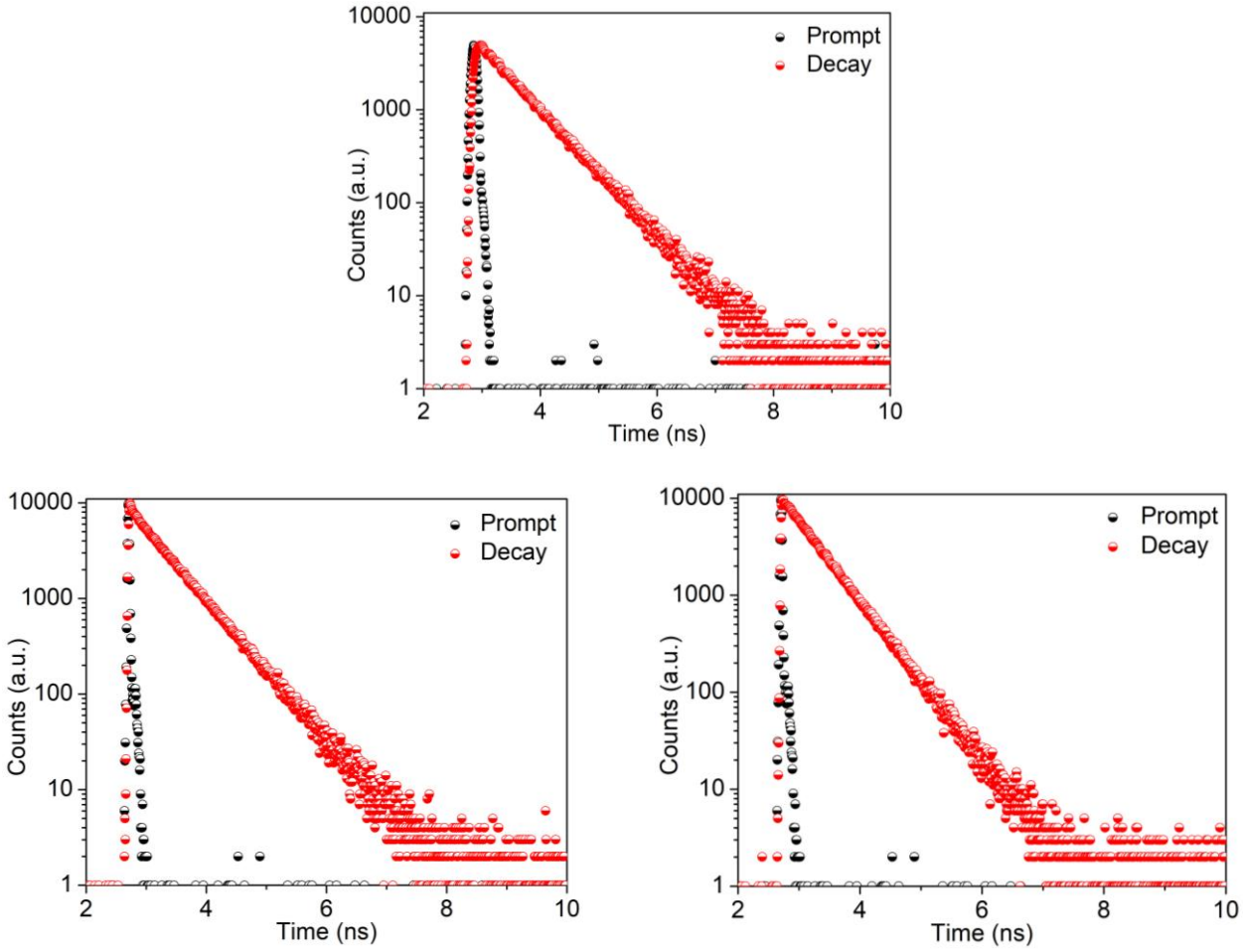

Fig. S10. Lifetime profiles of compounds **2** (top), **3** (bottom left) and **4** (bottom right) in cyclohexane solution.

VI. Mechanofluorochromic properties of compounds 2, 3YC, 3RC and 4

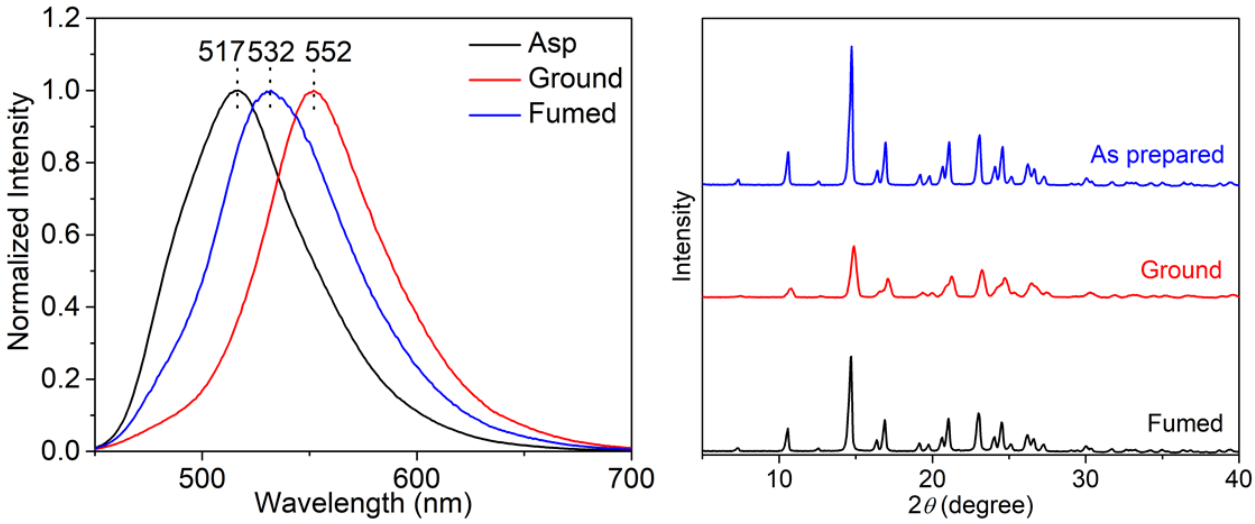

Fig. S11. Normalized PL spectra of **2** under different conditions (left) and Powder XRD diffractions of **2** under different conditions (right).

Fig. S12. Color changes of compound **2** upon grinding and fuming process under daylight.

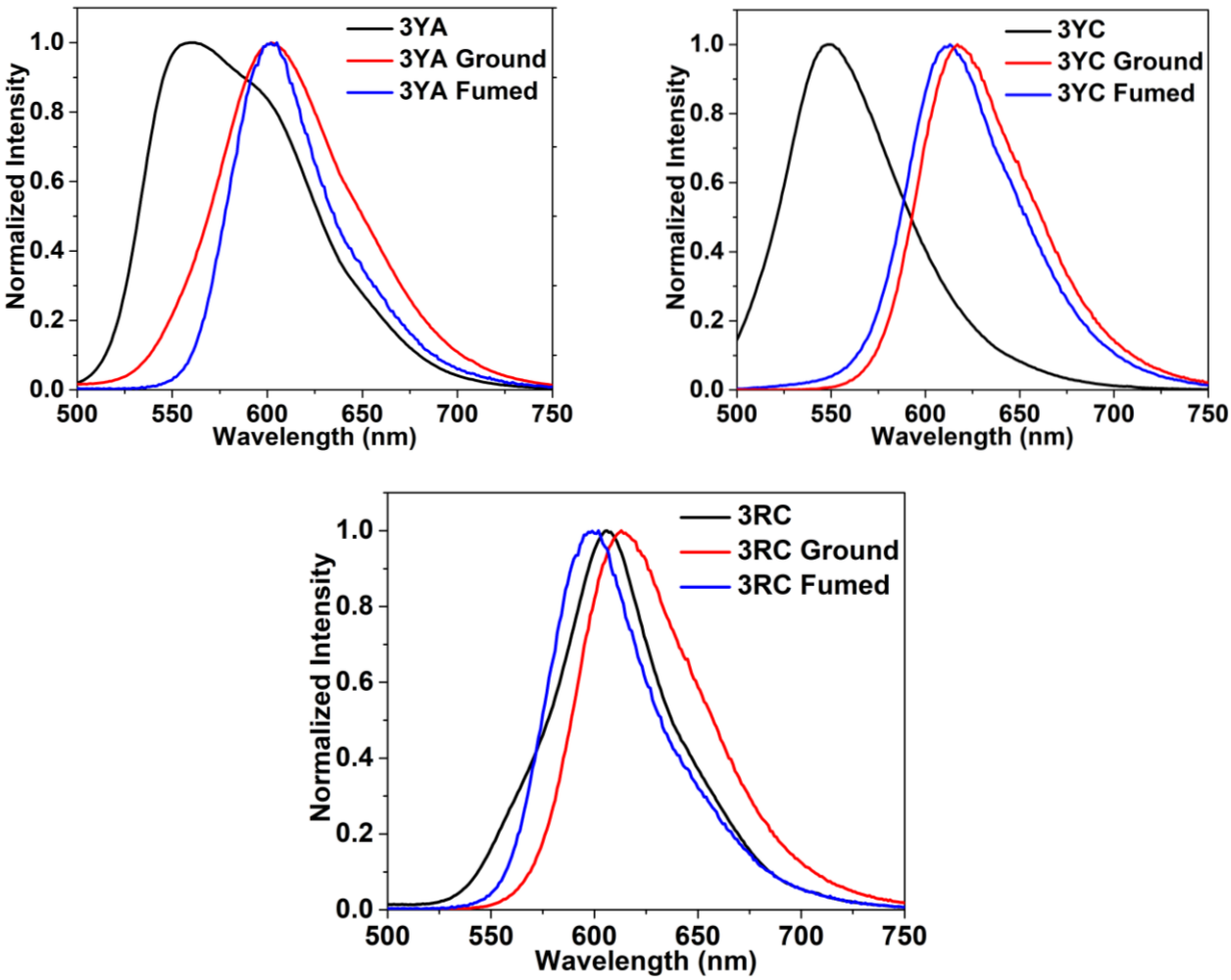

Fig. S13. Normalized PL spectra of **3YA** (top left), **3YC** (top right) and **3RC** (bottom) under different conditions.

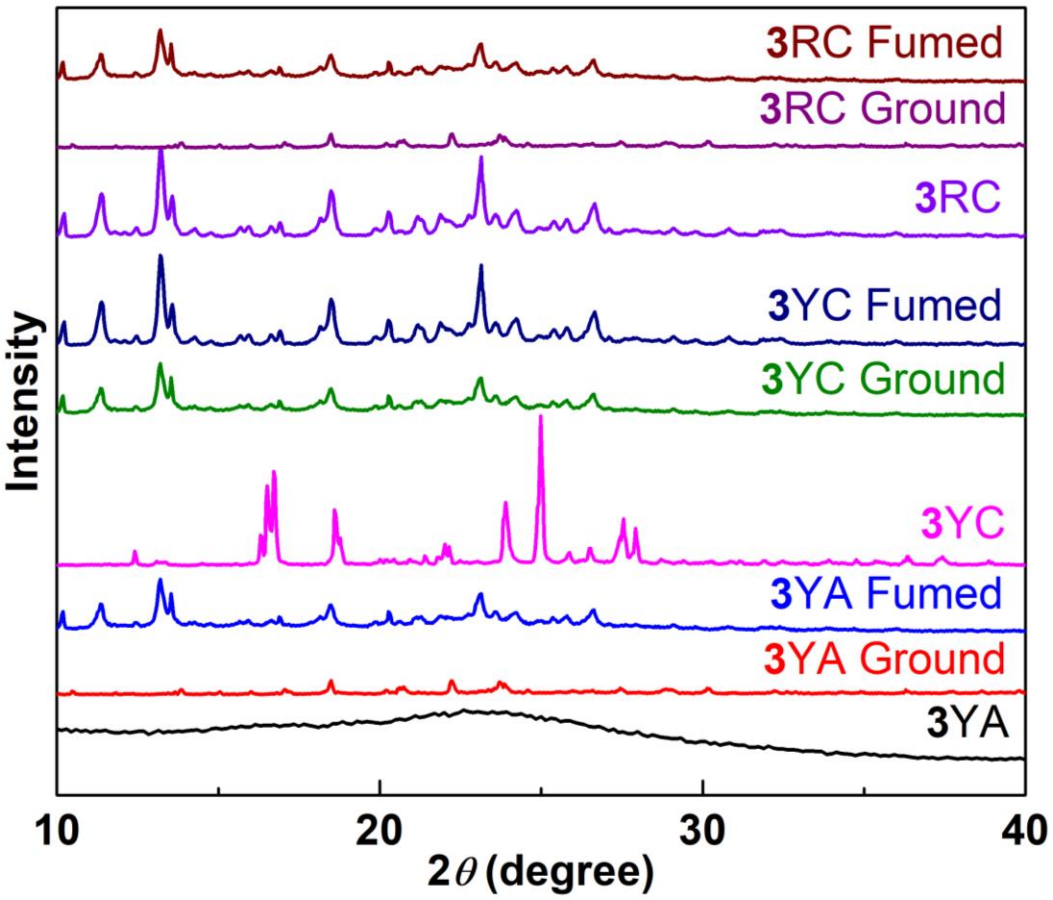

Fig. S14. Powder XRD diffractions of **3YA**, **3YC** and **3RC** under different conditions.

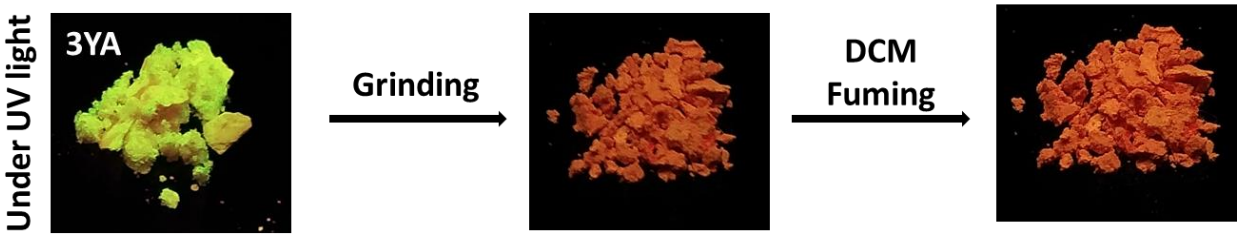

Fig. S15. Color changes of compound **3YA** upon grinding and fuming process under UV light irradiation at 365 nm.

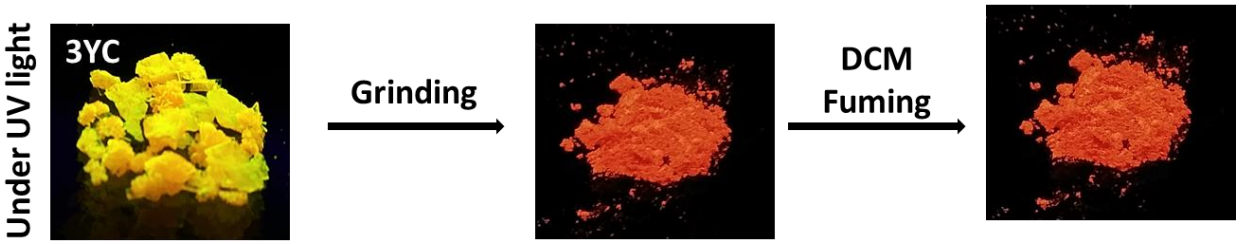

Fig. S16. Color changes of compound **3YC** upon grinding and fuming process under UV light irradiation at 365 nm.

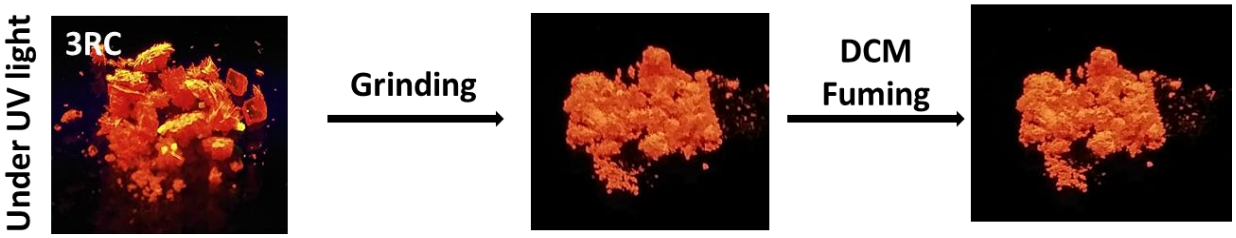

Fig. S17. Color changes of compound **3RC** upon grinding and fuming process under UV light irradiation at 365 nm.

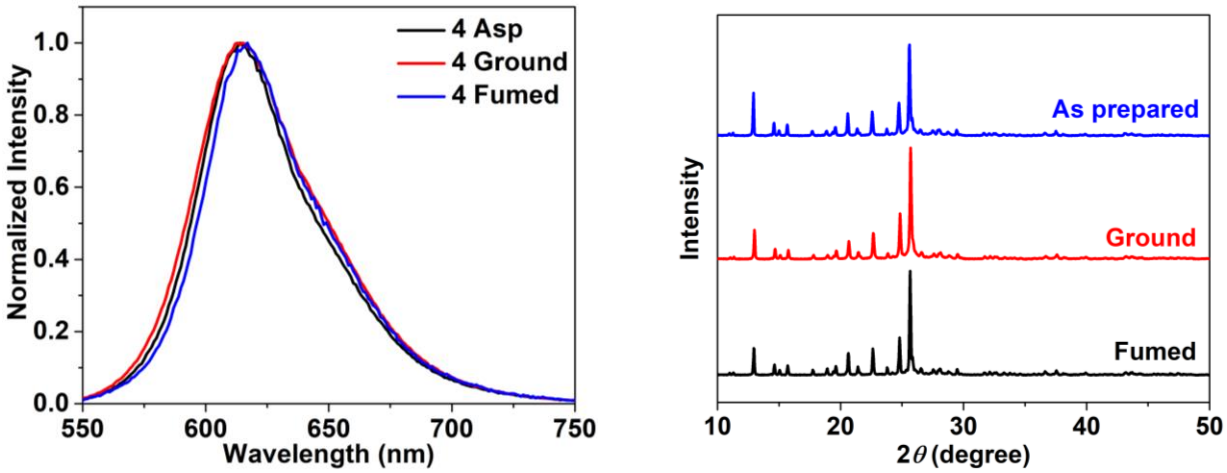

Fig. S18. Normalized PL spectra of **4** under different conditions (left) and Powder XRD diffractions of **4** under different conditions (right).

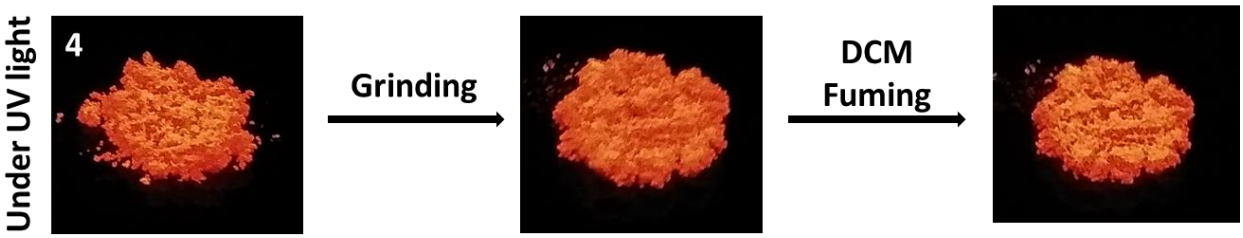

Fig. S19. Color changes of compound **4** upon grinding and fuming process under UV light irradiation at 365 nm.

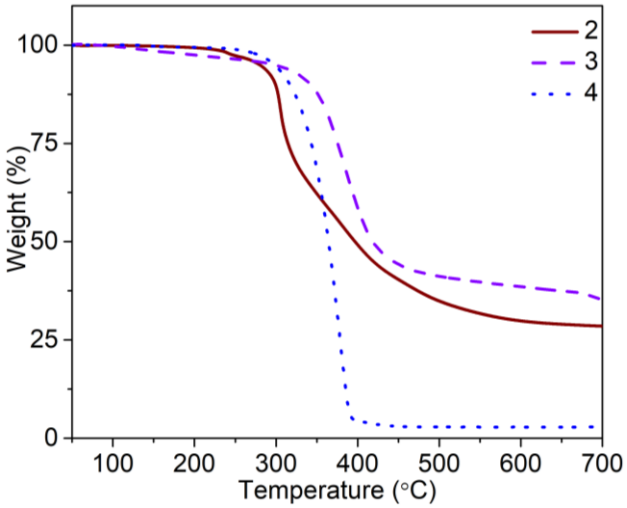

Fig. S20. TGA thermogram of **2**-**4** recorded under nitrogen at a heating rate of 10 °C min^{-1}.

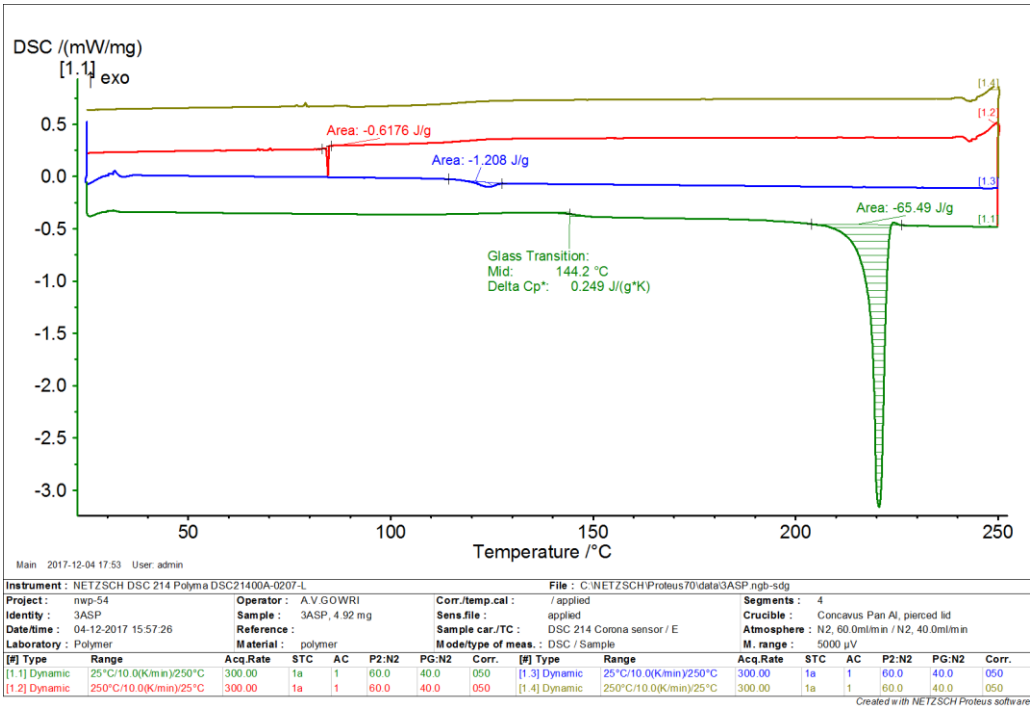

Fig. S21. DSC thermogram of as prepared compound **3** recorded under nitrogen at a scan rate of 10 °C min^{-1}.

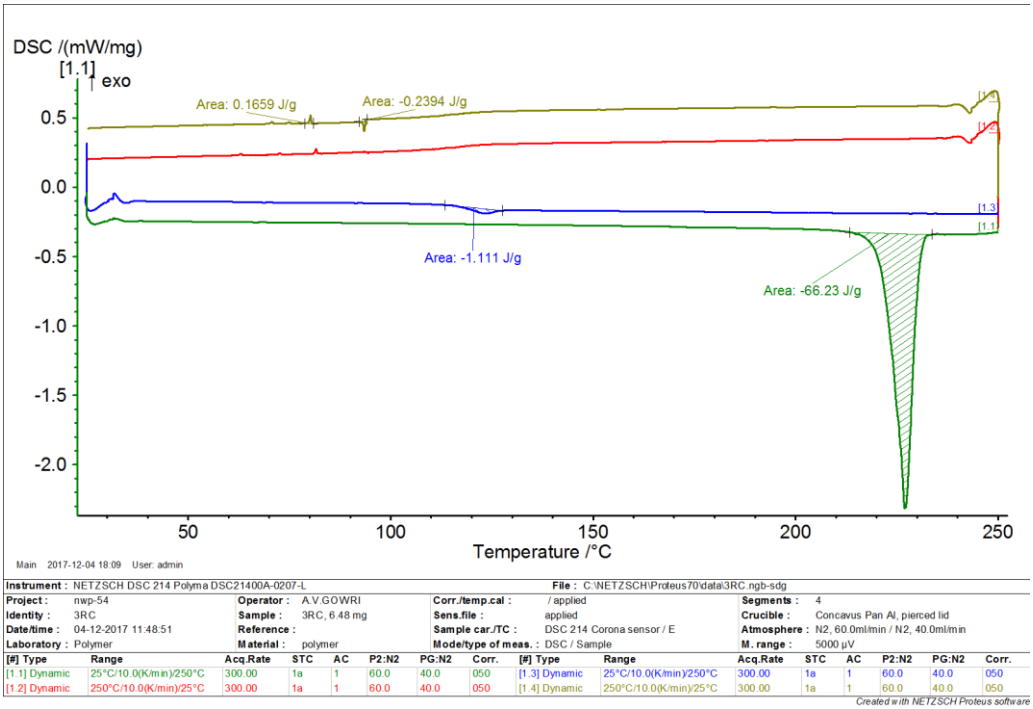

Fig. S22. DSC thermogram of **3RC** crystals recorded under nitrogen at a scan rate of 10 °C min^{-1}.

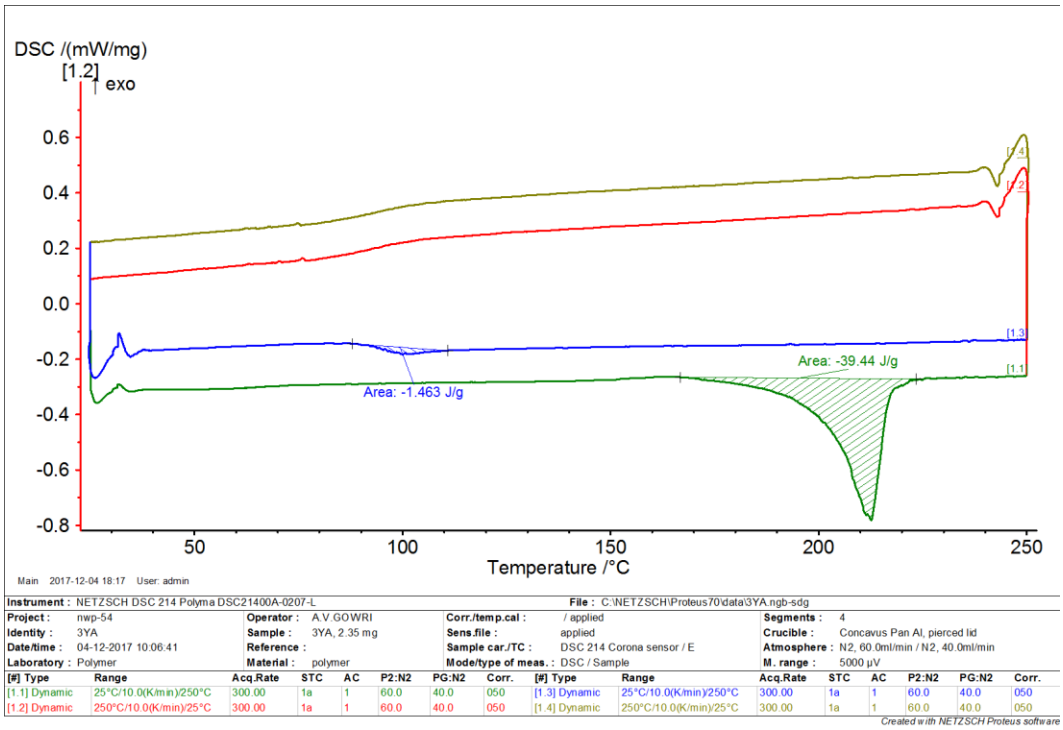

Fig. S23. DSC thermogram of **3YA** crystals recorded under nitrogen at a scan rate of 10 °C min^{-1}.

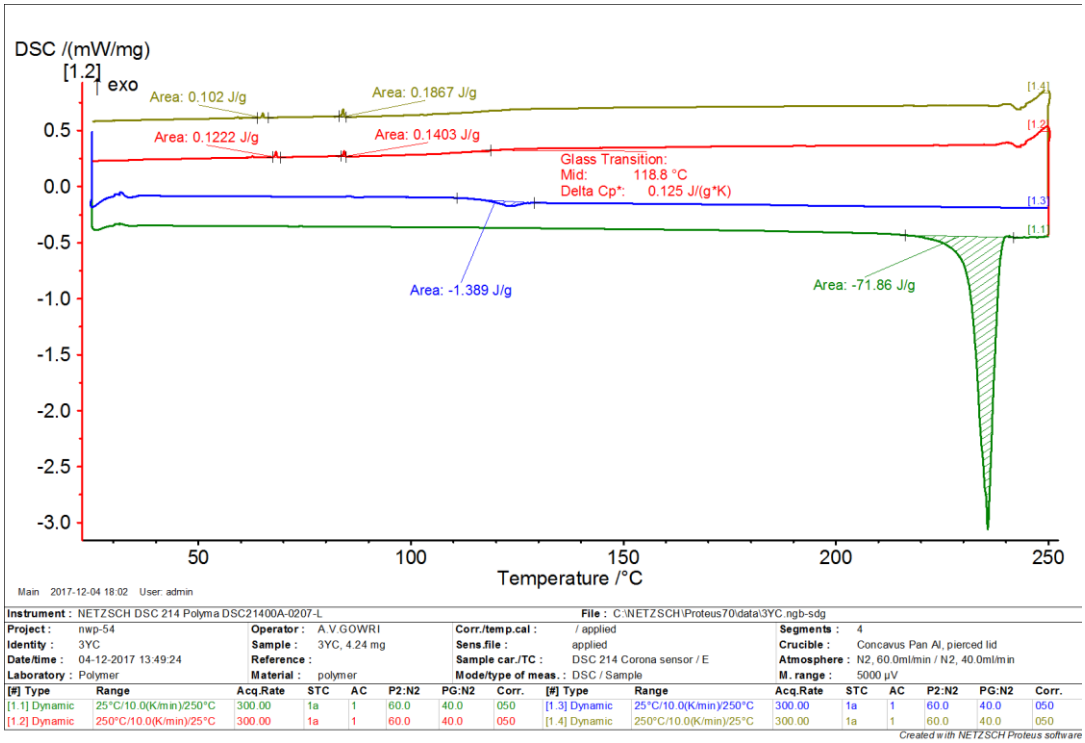

Fig. S24. DSC thermogram of **3YC** crystals recorded under nitrogen at a scan rate of 10 °C min^{-1}.

VII. X-ray Single Crystal Data and Their Packing Modes

Table S4. Crystallographic data collection and refinement parameter for **3YC**, **3RC** and **4**

Compounds	**3YC**	**3RC**	**4**
Empirical formula	$C_{41}H_{38}BBrN_2S$	$C_{41}H_{38}BBrN_2S$	$C_{23}H_{17}BrN_2S$
Formula weight	681.51	681.51	433.35
Temperature/K	293(2)	293(2)	293(2)
Crystal system	triclinic	monoclinic	monoclinic
Space group	P-1	$P2_1/c$	$P2_1/n$
a/Å	8.151(7)	9.6323(7)	10.5728(2)
b/Å	14.060(12)	13.5037(11)	13.7128(3)
c/Å	16.644(13)	52.648(4)	13.8757(3)
α/°	97.54(3)	90	90
β/°	93.66(3)	93.701(2)	108.5420(10)
γ/°	102.91(3)	90	90
Volume/Å^3	1835(3)	6833.7(9)	1907.31(7)
Z	2	8	4
ρ_{calc}g/cm^3	1.234	1.325	1.509
μ/mm^{-1}	1.207	1.296	2.275
F(000)	708	2832	880
Crystal size/mm^3	0.300 × 0.250 × 0.200	0.250 × 0.150 × 0.120	0.150 × 0.150 × 0.100
Radiation	MoKα (λ = 0.71073)	MoKα (λ = 0.71073)	MoKα (λ = 0.71073)
2Θ range for data collection/°	6.012 to 54.636	6.088 to 50	5.84 to 50
Index ranges	-10 ≤ h ≤ 10, -17 ≤ k ≤ 18, -21 ≤ l ≤ 21	-11 ≤ h ≤ 11, -16 ≤ k ≤ 16, -56 ≤ l ≤ 62	-12 ≤ h ≤ 12, -16 ≤ k ≤ 16, -16 ≤ l ≤ 16
Reflections collected	45663	83419	31753
Independent reflections	8114 [R_{int} = 0.0559, R_{sigma} = 0.0499]	11009 [R_{int} = 0.0624, R_{sigma} = 0.0799]	3348 [R_{int} = 0.0668, R_{sigma} = 0.0331]
Data/restraints/parameters	8114/0/418	11009/0/829	3348/0/244
Goodness-of-fit on F^2	1.018	1.132	1.132
Final R indexes [I>=2σ (I)]	R_1 = 0.0511, wR_2 = 0.1092	R_1 = 0.0774, wR_2 = 0.1302	R_1 = 0.0505, wR_2 = 0.1025
Final R indexes [all data]	R_1 = 0.1066, wR_2 = 0.1298	R_1 = 0.1186, wR_2 = 0.1415	R_1 = 0.0913, wR_2 = 0.1335
Largest diff. peak/hole / e Å^{-3}	0.43/-0.62	0.54/-0.62	0.67/-0.54
Crystal Pictures			

Single crystal X-ray structure and packing of the corresponding compounds

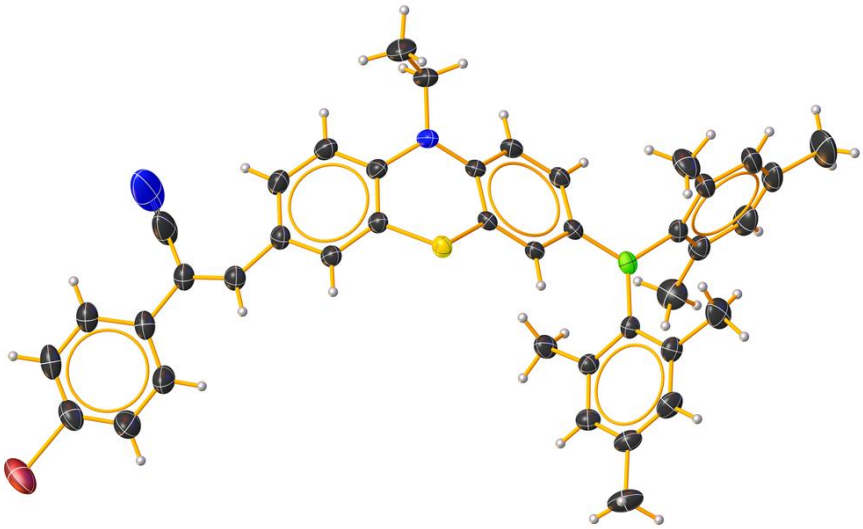

Fig. S25. The molecular structure of **3YC**. Atomic displacement ellipsoids are drawn at 50% probability. Disordered hydrogen atoms on the methyl groups have been removed for clarity. Color codes: black = carbon; grey = hydrogen; blue = nitrogen; green = boron; yellow = sulfur; brown = bromine.

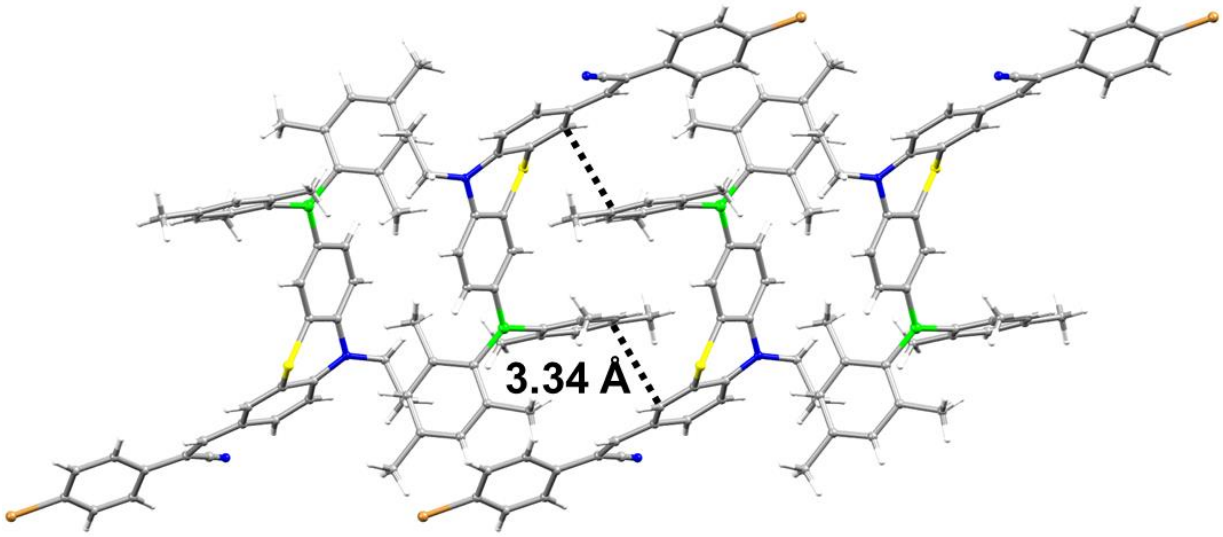

Fig. S26. Crystal packing mode as well as short contacts of **3YC**

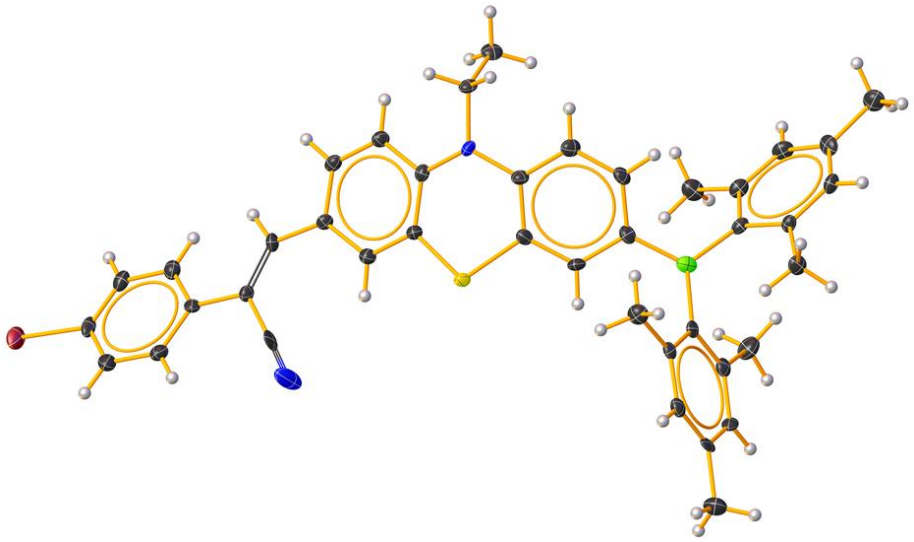

Fig. S27. The molecular structure of **3RC**. Atomic displacement ellipsoids are drawn at 50% probability. Disordered hydrogen atoms on the methyl groups have been removed for clarity. Color codes: black = carbon; grey = hydrogen; blue = nitrogen; green = boron; yellow = sulfur; brown = bromine.

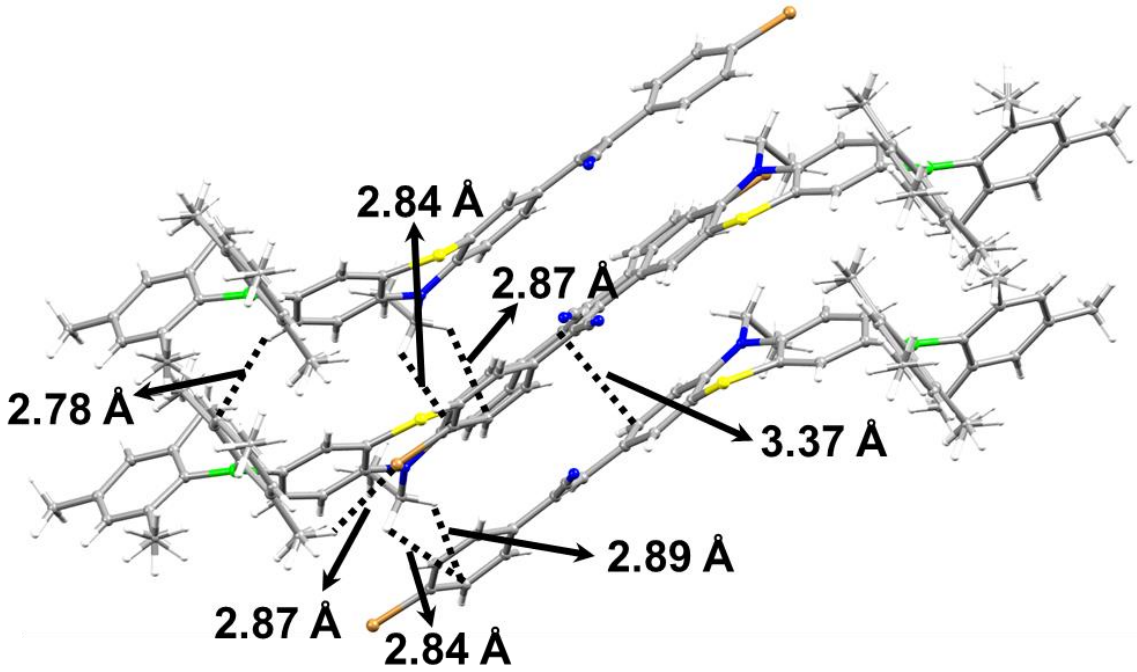

Fig. S28. Crystal packing mode as well as short contacts of **3RC**

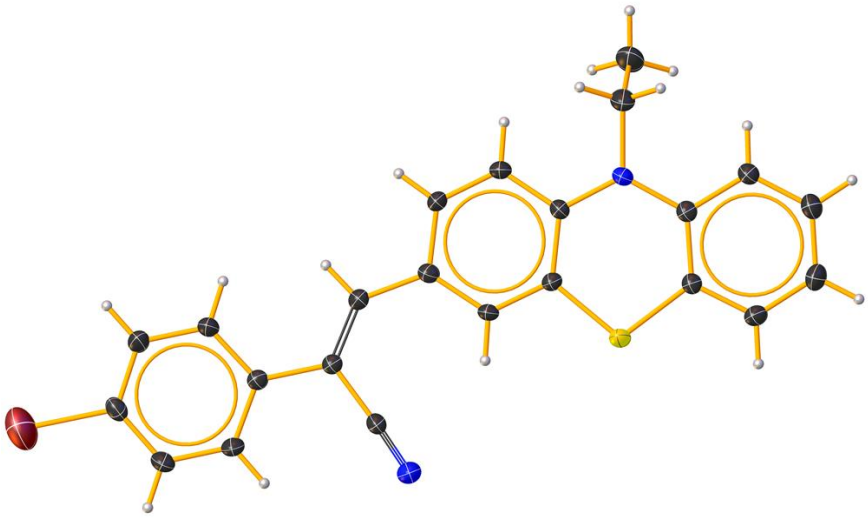

Fig. S29. The molecular structure of **4**. Atomic displacement ellipsoids are drawn at 30% probability. Color codes: black = carbon; grey = hydrogen; blue = nitrogen; yellow = sulfur; brown = bromine.

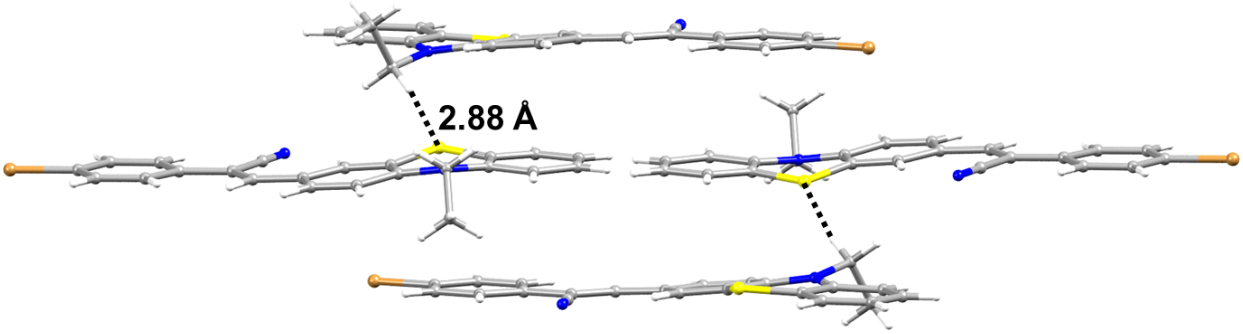

Fig. S30. Crystal packing mode as well as short contacts of **4**

Table S5. Intermolecular contacts details for **3YC**

Donor – H···Acceptor	D – H	H···A	D···A	D – H···A
C32-H32F…Cg(π)^{i}	0.96	2.77	3.626(2)	148
C28…π(C8)^{i}	-	-	3.34(4)	-

Symmetry codes: (i) 1-x, 2-y,1-z; Cg(π)= C7/C8/C9/C10/C11/C12

Table S6. Intermolecular contacts details for **3RC**

Donor – H···Acceptor	D – H	H···A	D···A	D – H···A
C74-H74…N4^{i}	0.93	2.59	3.436(3)	169
C33-H33…N2^{ii}	0.93	2.58	3.400(2)	166
C40-H40…N2^{ii}	0.93	2.60	3.486(2)	159
C25-H25A…π(C79)^{ii}	0.97	2.84	3.432(2)	120
C25-H25B…π(C80)^{ii}	0.97	2.88	3.336(2)	110
C66-H66A…π(C39)^{iii}	0.97	2.84	3.24(2)	105
C66-H66B…π(C40)^{iii}	0.97	2.89	3.24(2)	102
C24-H24…π(C44)^{iv}	0.97	2.78	3.636(2)	153

Symmetry codes: (i) 1-x, ½+y, ½-z; (ii) -x, ½+y, ½-z; (iii) -x, -½+y, ½-z; (i) -1+x, 1+y, z

Table S7. Intermolecular contacts details for **4**

Donor – H···Acceptor	D – H	H···A	D···A	D – H···A
C11-H11...N1	0.93	2.62	3.453(6)	150
C22-H22A...S1^{i}	0.97	2.89	3.835(6)	166

Symmetry codes: (i) -x+½, y+½, -z+3/2

VIII. Plots of ^{1}H, $^{11}B\{^{1}H\}$, and $^{13}C\{^{1}H\}$ NMR Spectra

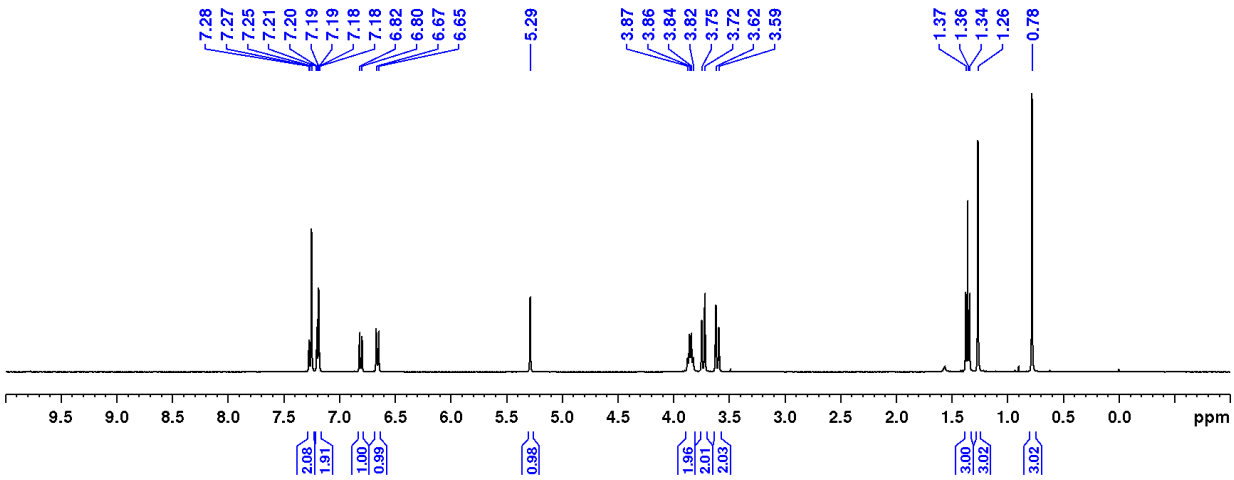

^{1}H NMR spectrum of **1** ($CDCl_3$, 400 MHz).

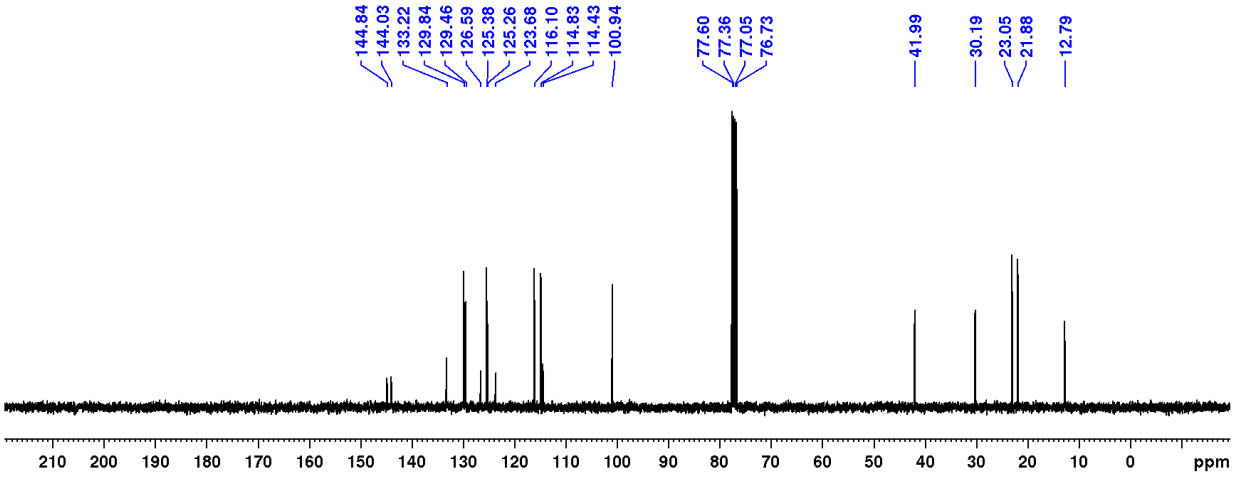

$^{13}C\{^{1}H\}$ NMR spectrum of **1** ($CDCl_3$, 100 MHz).

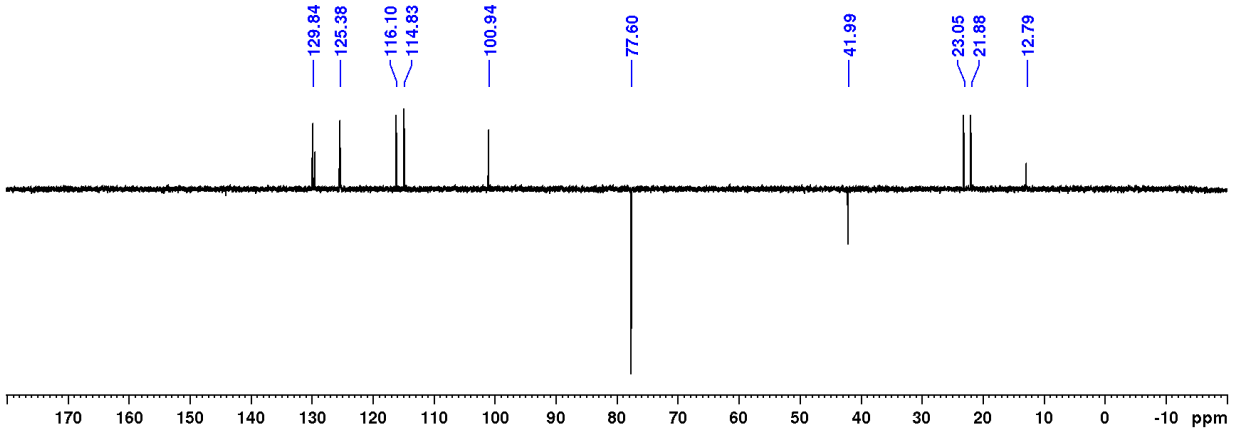

$^{13}C\{^{1}H\}$ DEPT-135 NMR spectrum of **1** ($CDCl_3$, 100 MHz).

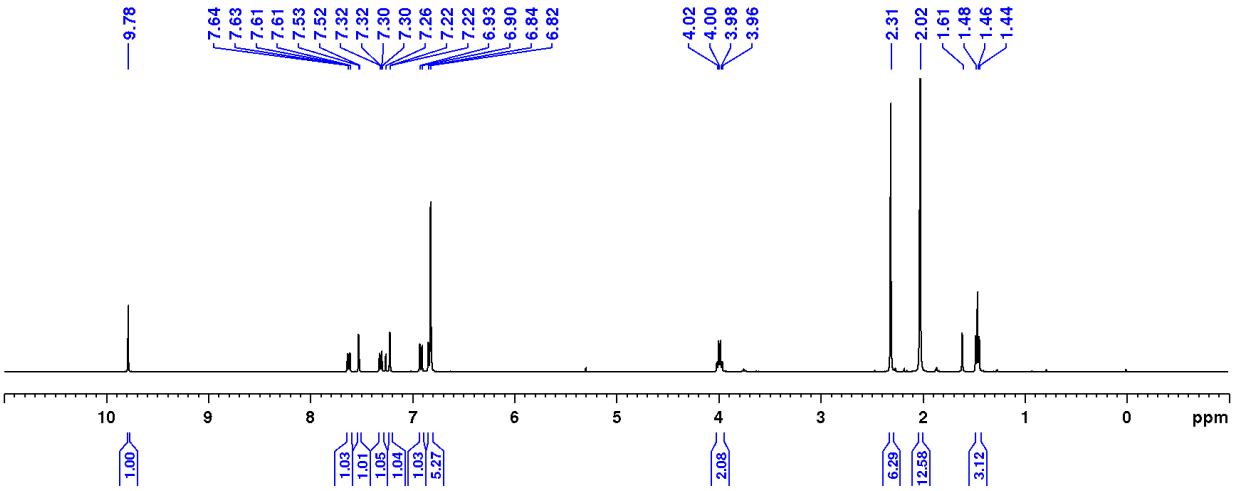

^{1}H NMR spectrum of **2** ($CDCl_3$, 400 MHz).

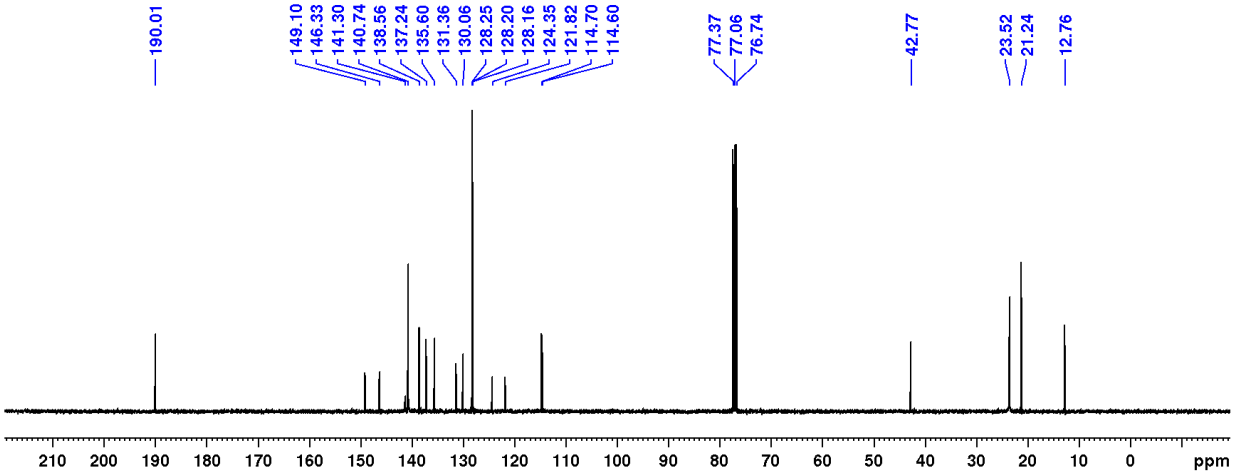

$^{13}C\{^{1}H\}$ NMR spectrum of **2** ($CDCl_3$, 100 MHz).

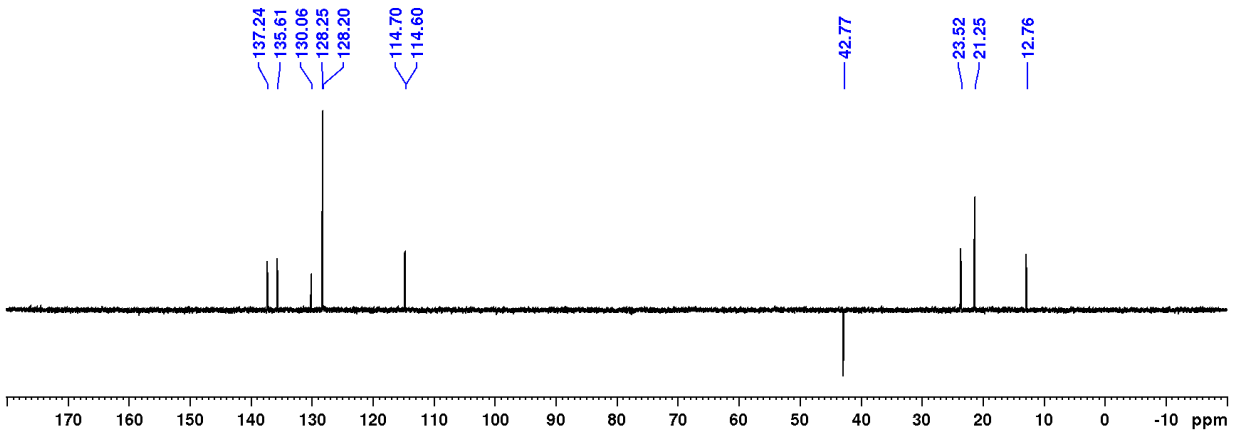

$^{13}C\{^{1}H\}$ DEPT-135 NMR spectrum of **2** ($CDCl_3$, 100 MHz).

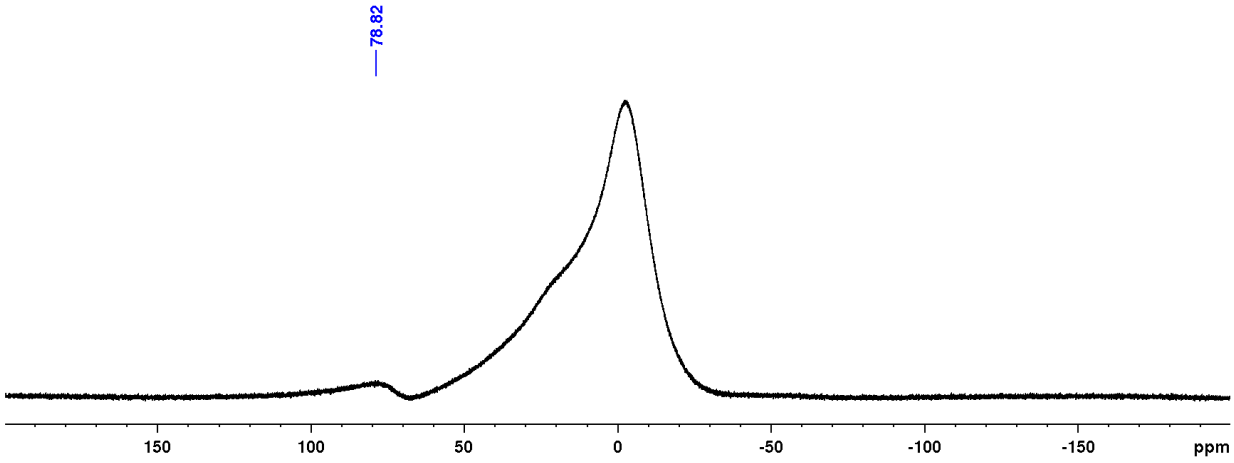

$^{11}B\{^{1}H\}$ NMR spectrum of **2** ($CDCl_3$, 160 MHz).

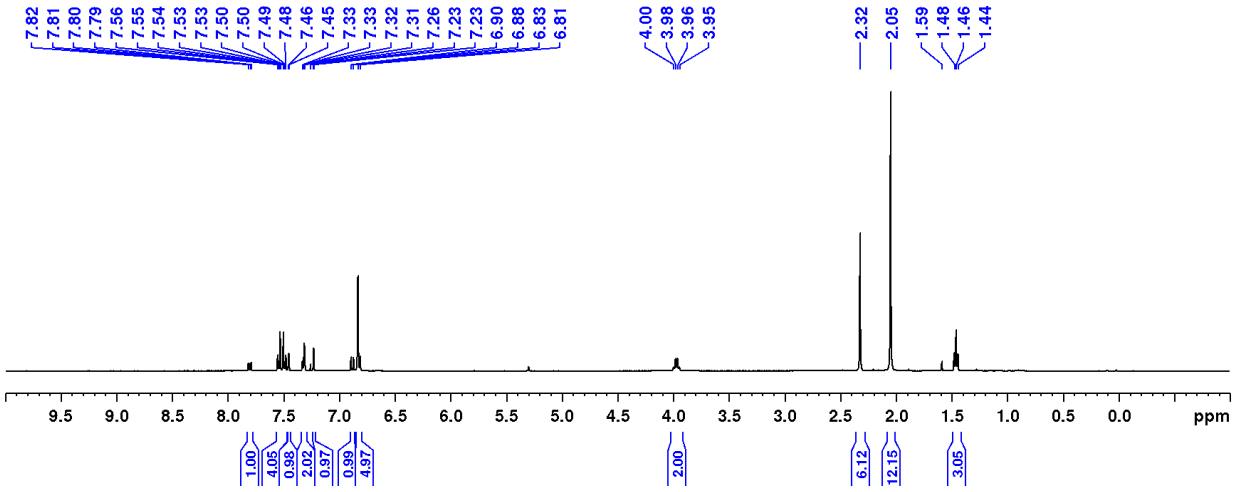

^{1}H NMR spectrum of **3** ($CDCl_3$, 400 MHz).

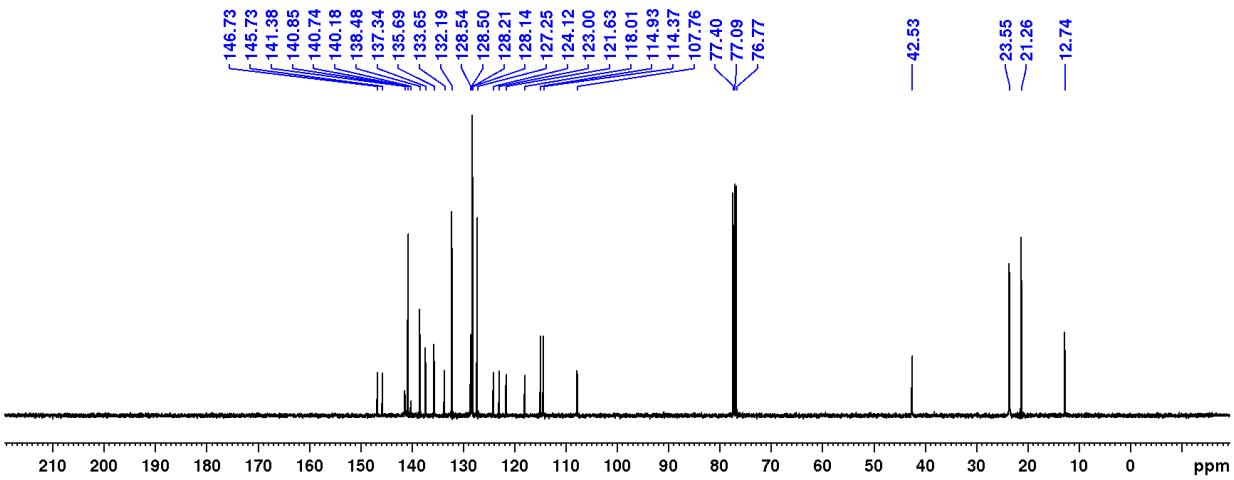

$^{13}C\{^{1}H\}$ NMR spectrum of **3** ($CDCl_3$, 100 MHz).

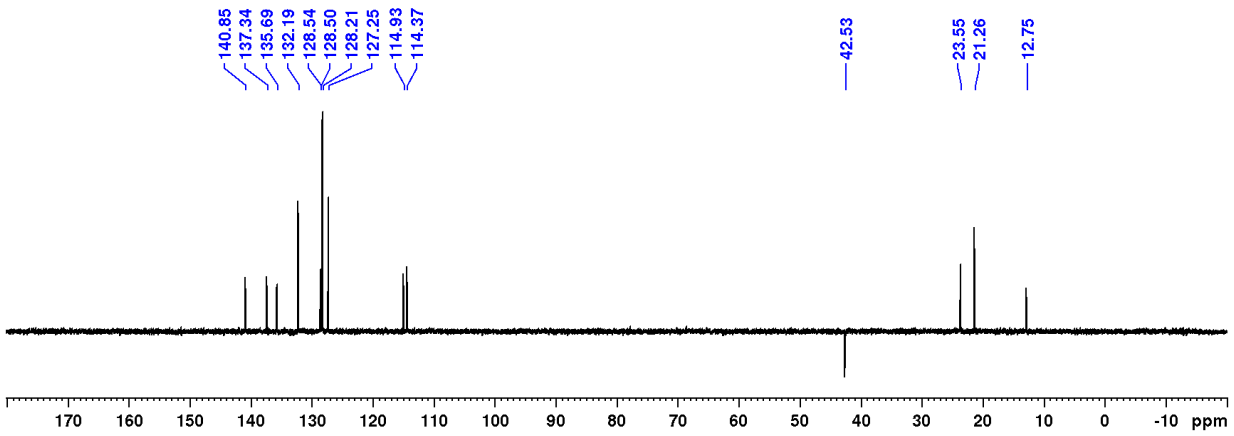

$^{13}C\{^{1}H\}$ DEPT-135 NMR spectrum of **3** ($CDCl_3$, 100 MHz).

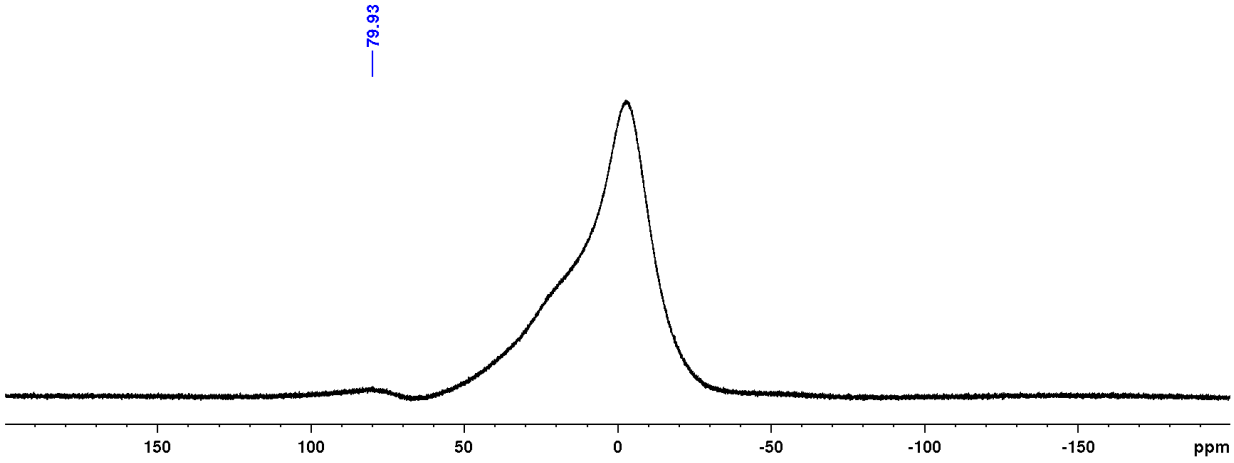

$^{11}B\{^{1}H\}$ NMR spectrum of **3** ($CDCl_3$, 160 MHz).

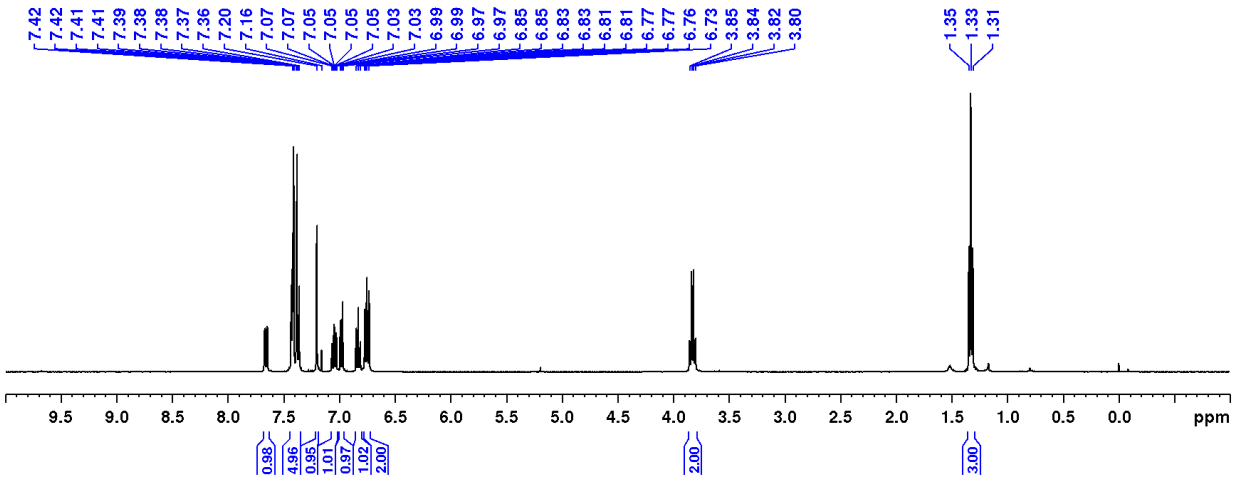

^{1}H NMR spectrum of **4** ($CDCl_3$, 400 MHz).

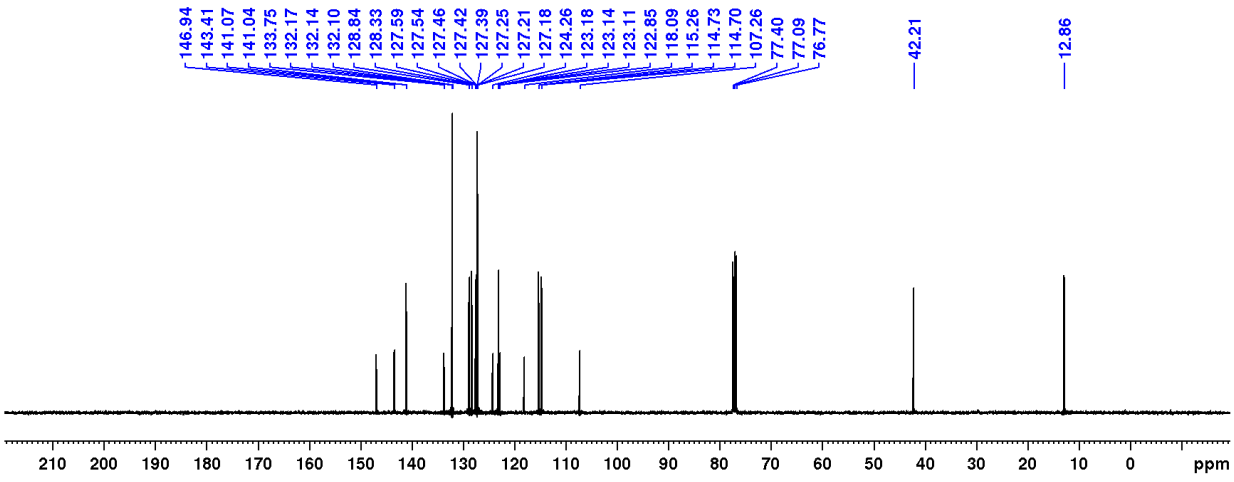

$^{13}C\{^{1}H\}$ NMR spectrum of **4** ($CDCl_3$, 100 MHz).

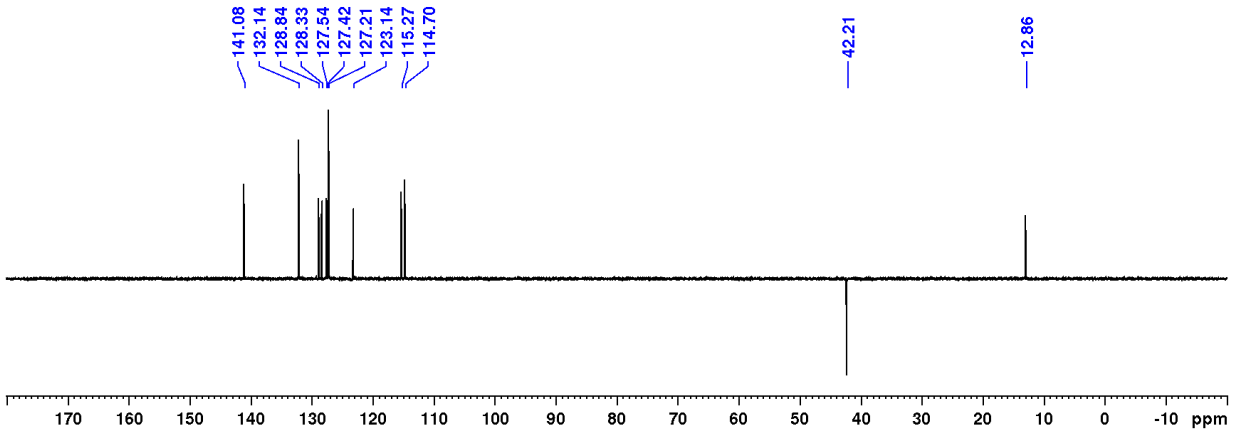

$^{13}C\{^{1}H\}$ DEPT-135 NMR spectrum of **4** ($CDCl_3$, 100 MHz).

IX. HRMS data for compounds 2-4.

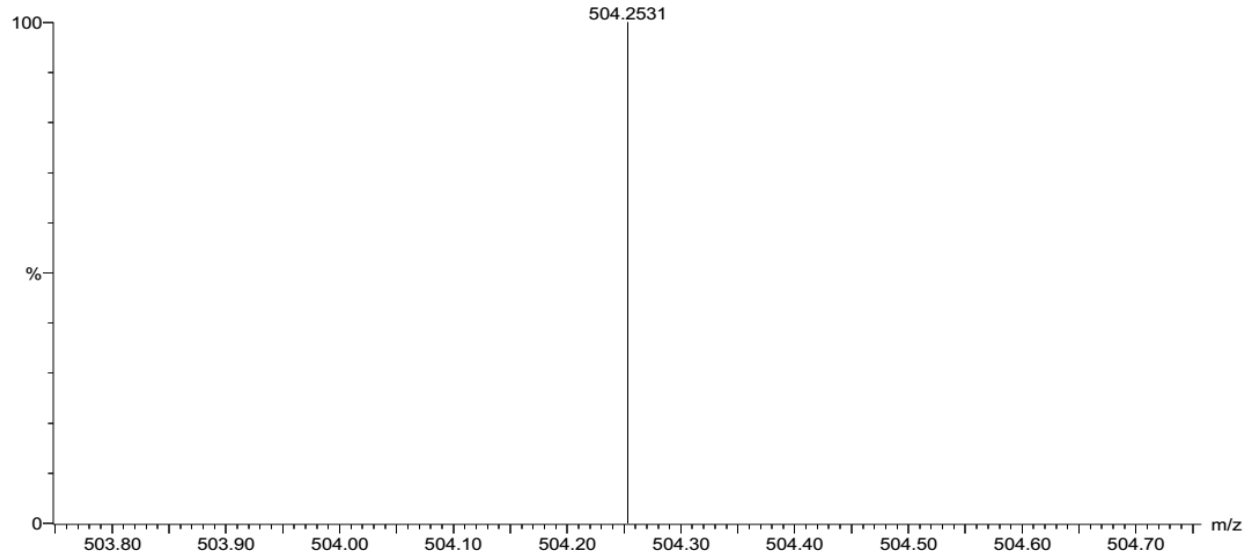

Minimum:				-1.5		
Maximum:		5.0	10.0	50.0		
Mass	Calc. Mass	mDa	PPM	DBE	i-FIT	Formula
504.2531	504.2532	-0.1	-0.2	17.5	n/a	C33 H35 B N O S

HRMS spectrum of compound **2**

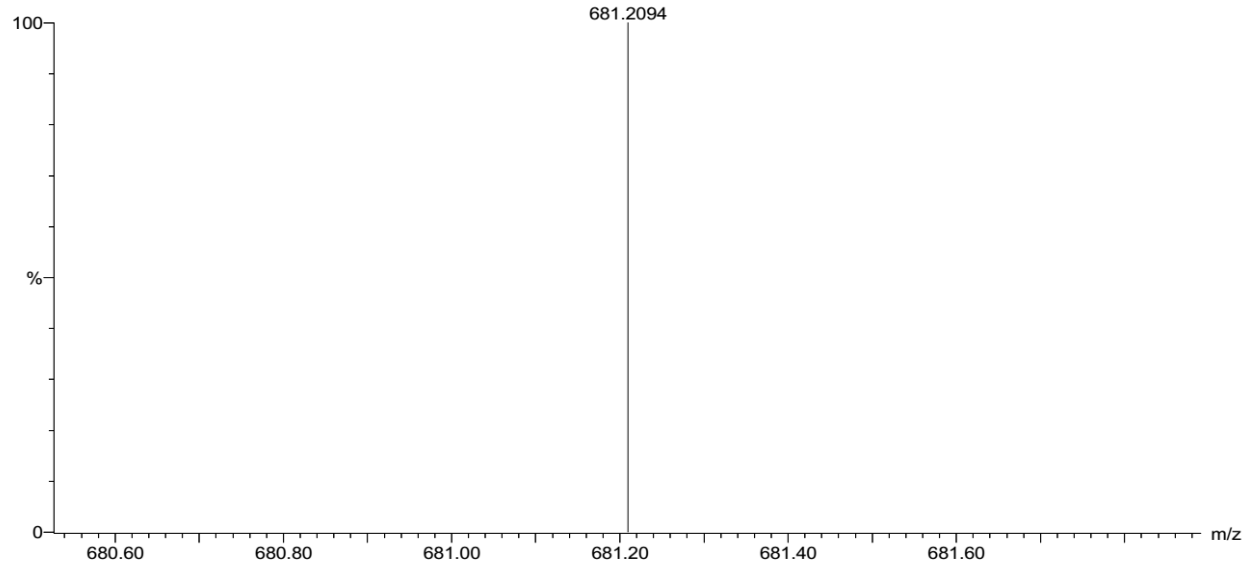

Minimum:				-1.5		
Maximum:		5.0	10.0	50.0		
Mass	Calc. Mass	mDa	PPM	DBE	i-FIT	Formula
681.2094	681.2110	-1.6	-2.3	23.5	n/a	C41 H39 B N2 S Br

HRMS spectrum of compound **3**

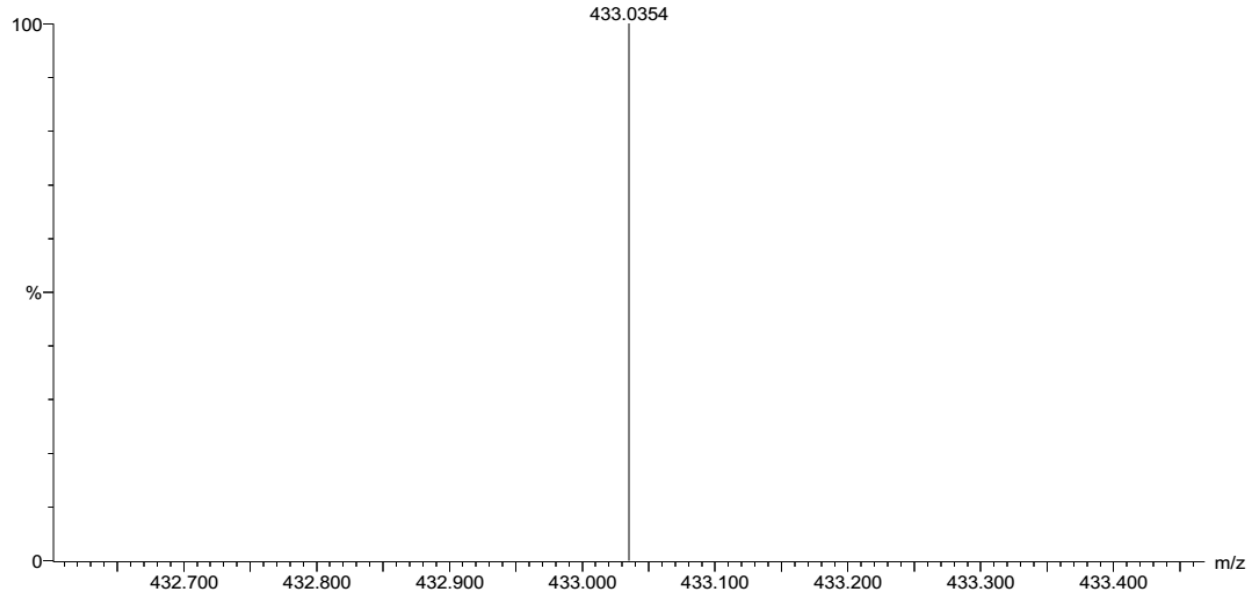

Minimum:				-1.5		
Maximum:		5.0	10.0	50.0		
Mass	Calc. Mass	mDa	PPM	DBE	i-FIT	Formula
433.0354	433.0374	-2.0	-4.6	15.5	n/a	C23 H18 N2 S Br

HRMS spectrum of compound **4**

X. References:

1. A. Ito, Y. Kang, S. Saito, E. Sakuda, N. Kitamura, *Inorg. Chem.,* **2012**, *51*, 7722–7732.
2. Z. Iqbal, W.-Q. Wu, H. Zhang, P.-L. Hua, X. Fang, D.-B. Kuang, L. Wang, H. Meier, D. Cao, *Dyes Pigm.,* **2013,** *99*, 299-307.
3. SMART/SAINT; Bruker AXS, Inc., Madison, WI, **2004**.
4. G. M. Sheldrick, SADABS, Bruker Nonius Area Detector Scaling and Absorption Correction, version 2.05; University of Gottingen: Gottingen, Germany, **1999**.
5. G. M. Sheldrick, SHELXL-2014/7: *Program for the Solution of Crystal Structures*, University of Gottingen, GÖttingen, Germany, 2014.
6. M. J. Frisch, G. W. Trucks, H. B. Schlegel, G. E. Scuseria, M. A. Robb, J. R. Cheeseman, G. Scalmani, V. Barone, B. Mennucci, G. A. Petersson, H. Nakatsuji, M. Caricato, X. Li, H. P. Hratchian, A. F. Izmaylov, J. Bloino, G. Zheng, J. L. Sonnenberg, M. Hada, M. Ehara, K. Toyota, R. Fukuda, J. Hasegawa, M. Ishida, T. Nakajima, Y. Honda, O. Kitao, H. Nakai, T. Vreven, J. A. Montgomery, Jr., J. E. Peralta, F. Ogliaro, M. Bearpark, J. J. Heyd, E. Brothers, K. N. Kudin, V. N. Staroverov, T. Keith, R. Kobayashi, J. Normand, K. Raghavachari, A. Rendell, J. C. Burant, S. S. Iyengar, J. Tomasi, M. Cossi, N. Rega, J. M. Millam, M. Klene, J. E. Knox, J. B. Cross, V. Bakken, C. Adamo, J. Jaramillo, R. Gomperts, R. E. Stratmann, O. Yazyev, A. J. Austin, R. Cammi, C. Pomelli, J. W. Ochterski, R. L. Martin, K. Morokuma, V. G. Zakrzewski, G. A. Voth, P. Salvador, J. J. Dannenberg, S. Dapprich, A. D. Daniels, O. Farkas, J. B. Foresman, J. V. Ortiz, J. Cioslowski, D. J. Fox, Gaussian, Inc., Wallingford CT, 2010.
7. a) A. D. Becke, *J. Chem. Phys.,***1993**, *98*, 5648–5652; b) C. Lee, W. Yang, R. G. Parr, *Phys. Rev., B* **1988**, *37*, 785–789; c) P. J. Stephens, F. J. Devlin, C. F. Chabalowski, M. J. Frisch, *J. Phys. Chem.* **1994**, *98*, 11623–11627.
8. a) G. A. Petersson, M. A. Al-Laham, *J. Chem. Phys.,* **1991**, 94, 6081–6090; b) G. A. Petersson, A. Bennett, T. G. Tensfeldt, M. A. Al-Laham, W. A. Shirley, J. Mantzaris, *J. Chem. Phys.,* **1988**, *89*, 2193–2218.
9. T. Yanai, D. P. Tew, N. C. Handy, *Chem. Phys. Lett.,* **2004**, *393*, 51–57.
10. N. M. O'Boyle, A. L. Tenderholt and K. M. Langner, *J. Comput. Chem.,* 2008, **29***,* 839–845.